

# Chapter 2—Outline

## Exact Ray Tracing and Spherical Aberration

|  |    |
|--|----|
| <b>Chapter 2: Exact Ray Tracing and Spherical Aberration</b> . . . . .                           | 63 |
| <b>2.1 Introduction</b> . . . . .  | 63 |
| <b>2.2 Skew Ray Description and Vectors</b> . . . . .  | 63 |
| <b>2.2.1 Direction angles and direction cosines</b> . . . . .                                    | 63 |
| Example 2.2.1 Vector on the $z$ axis . . . . .   | 64 |
| Example 2.2.2 Vector on the $-z$ axis . . . . .  | 64 |
| Example 2.2.3 Vector not parallel to any of the axes . . . . .                                   | 65 |
| Example 2.2.4 Vector given by its components . . . . .   | 65 |
| <b>2.2.2 The dot product</b> . . . . .   | 66 |
| Example 2.2.5 Calculation of the angle between two vectors in three dimensions . . . . .         | 66 |
| <b>2.2.3 The cross product</b> . . . . .   | 67 |
| <b>2.3 Exact Ray Tracing of Skew Rays</b> . . . . .  | 68 |
| <b>2.3.1 The translation equations</b> . . . . .   | 68 |
| A closer look at $\mathbf{r} \cdot \mathbf{u} =  \mathbf{r}   \mathbf{u}  \cos \theta$ . . . . . | 70 |
| <b>2.3.2 The refraction equations</b> . . . . .  | 71 |
| <b>2.3.3 Summary of equations and application</b> . . . . .                                      | 73 |
| Example 2.3.1 Exact ray tracing of a skew ray . . . . .  | 73 |
| <b>2.4 Spherical Aberration</b> . . . . .  | 75 |
| <b>2.4.1 Equations for description</b> . . . . .   | 75 |
| Example 2.4.1 Spherical aberration in a biconvex lens . . . . .                                  | 75 |
| Example 2.4.2 The planoconvex lens . . . . .   | 76 |
| 1) Convex surface faces incident rays . . . . .  | 76 |
| 2) Plane surface faces incident rays . . . . .   | 77 |
| Comparison of the two orientations . . . . .   | 77 |
| Example 2.4.3 A single surface . . . . .   | 78 |
| <b>2.4.2 Shaping (or bending) a lens</b> . . . . .   | 78 |
| Example 2.4.4 Investigation of TSA versus $S$ . . . . .  | 79 |
| <b>2.4.3 The radius of a converging lens</b> . . . . .   | 80 |
| Example 2.4.5 Radius of a biconvex lens . . . . .  | 81 |
| Example 2.4.6 Radius of a planoconvex lens . . . . .   | 81 |
| Example 2.4.7 Radius of a shaped biconvex lens . . . . .   | 81 |
| Example 2.4.8 Radius of the biconvex lens used in the next section . . . . .                     | 81 |
| <b>2.4.4 Spherical aberration of a doublet</b> . . . . .   | 82 |
| 1) Lens with minimum $ TSA $ . . . . .   | 82 |
| 2) A doublet . . . . .   | 82 |
| 3) Summary . . . . .   | 83 |
| <b>Problems</b> . . . . .  | 83 |
| <b>Answers to Problems</b> . . . . .   | 86 |
| <b>References</b> . . . . .  | 87 |

**Page intentionally left blank.**

# Chapter 2

## Exact Ray Tracing and Spherical Aberration

### 2.1 Introduction

In Chapter 1 we described how paraxial rays—rays that travel close to the symmetry axis—pass through one or many spherical refracting surfaces, and how such rays travel from an object point to form an image point. It is interesting to note that paraxial mathematics is a consistent set of rules that describes rays even when they travel far from the symmetry axis and form large angles with their reference lines. However, such rays represent the paths followed by real rays rather poorly. Paraxial rays that have angles of inclination of about 6 deg or less describe real rays to approximately 3 significant figures. As rays deviate from the paraxial requirement, they can miss the image point appreciably to produce a blurred image. The term “aberration” denotes the behavior of rays in producing a blurred image.

To study these ray aberrations, we need a method that describes exactly—here, “exactly” means “equations without approximation”—what happens to a ray, paraxial or non-paraxial, when it translates between and passes through (centered) spherical refracting surfaces. Furthermore, the ray can travel in one, two, or three dimensions (that is, in any forward direction); such a ray is called a skew ray. In this chapter, we derive equations that describe exactly the path followed by skew rays, and utilize these equations with numerical methods to depict the aberration called spherical aberration.

### 2.2 Skew Ray Description and Vectors

To obtain the exact equations in this chapter that apply to three-dimensional ray travel, we use vectors because it makes the derivations easier. However, the algebra involved is still rather demanding. We develop some of the basic ideas we need in this section. To obtain a righthanded coordinate system consistent with the  $y$  and  $z$  axes we have been using, we point the  $x$  axis into the page.

#### 2.2.1 Direction angles and direction cosines

The direction of any directed line segment, or vector  $\mathbf{v}$ , is specified by the direction angles  $A$ ,  $B$ ,  $C$ , as shown in Figure 2.1. In this diagram, the vector has its tail at the origin  $O$ ,

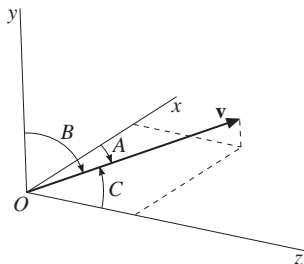


Figure 2.1

and the direction angles are measured relative to their respective  $x$ ,  $y$ ,  $z$  axes. However, the vector tail can be located anywhere, and the direction angles are still the same as shown in Figure 2.2.

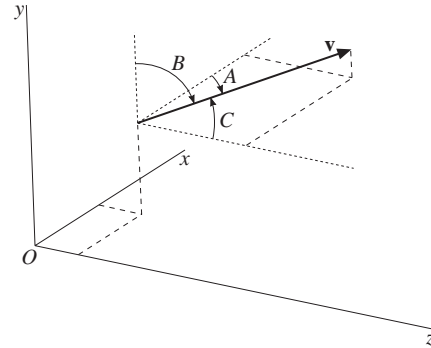


Figure 2.2

The direction cosines are defined as the cosines of the direction angles, namely:

$$\alpha = \cos A, \quad \beta = \cos B, \quad \gamma = \cos C \quad (2.1)$$

To obtain an important property of the direction cosines, we take the vector  $\mathbf{v}$  of Figure 2.2, along with its direction angles, and draw a box so that  $\mathbf{v}$  is one of the diagonals, as shown in Figure 2.3. Labeling the sides of the box as shown, we see by inspection that the magnitude  $|\mathbf{v}|$  (or more simply,  $v$ ) of the vector  $\mathbf{v}$  is, by Pythagorean’s theorem,

$$v = |\mathbf{v}| = \sqrt{(x_2 - x_1)^2 + (y_2 - y_1)^2 + (z_2 - z_1)^2} \quad (2.2)$$

Remembering that the cosine is defined as the side adjacent to the angle divided by the hypotenuse, we have

$$\alpha = \cos A = \frac{x_2 - x_1}{|\mathbf{v}|} \quad (2.3a)$$

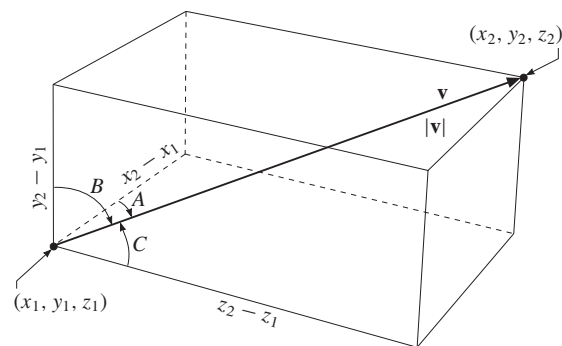


Figure 2.3

In a similar manner, we obtain for the direction cosines of the direction angles  $B$  and  $C$ :

$$\beta = \cos B = \frac{y_2 - y_1}{|\mathbf{v}|} \quad (2.3b)$$

$$\gamma = \cos C = \frac{z_2 - z_1}{|\mathbf{v}|} \quad (2.3c)$$

Using Equation 2.2 and Equations 2.3, we obtain the important identity that all direction cosines must obey:

$$\begin{aligned} \alpha^2 + \beta^2 + \gamma^2 &= \frac{(x_2 - x_1)^2}{|\mathbf{v}|^2} + \frac{(y_2 - y_1)^2}{|\mathbf{v}|^2} + \frac{(z_2 - z_1)^2}{|\mathbf{v}|^2} \\ &= \frac{|\mathbf{v}|^2}{|\mathbf{v}|^2} \\ &= 1 \end{aligned} \quad (2.4)$$

Equation 2.4 says that only two of the three direction cosines are independent; once two of the direction cosines (or direction angles) have been chosen, the third one is determined to within two choices. For example, suppose  $\alpha$  and  $\beta$  are given; then we can solve for  $\gamma$  to get  $\pm\sqrt{1 - \alpha^2 - \beta^2}$ . For rays that are forward directed, we would choose the plus sign.

A unit vector is defined to be a vector of unit magnitude. In Figure 2.4,  $\mathbf{u}$  is a unit vector parallel to the vector  $\mathbf{v}$ , and  $\mathbf{i}, \mathbf{j}, \mathbf{k}$  are unit vectors parallel to the  $x, y, z$  axes, respectively. Unit vectors  $\mathbf{u}$  are expressed in terms of the direction cosines; for example, by inspection of Figure 2.4, we have

$$\begin{aligned} \mathbf{u} &= \frac{\mathbf{v}}{|\mathbf{v}|} = \frac{(x_2 - x_1)\mathbf{i} + (y_2 - y_1)\mathbf{j} + (z_2 - z_1)\mathbf{k}}{|\mathbf{v}|} \\ &= \frac{(x_2 - x_1)}{|\mathbf{v}|}\mathbf{i} + \frac{(y_2 - y_1)}{|\mathbf{v}|}\mathbf{j} + \frac{(z_2 - z_1)}{|\mathbf{v}|}\mathbf{k} \\ &= \alpha\mathbf{i} + \beta\mathbf{j} + \gamma\mathbf{k} \end{aligned} \quad (2.5)$$

where in the last step, we have used Equations 2.3. All unit vectors have this efficient representation in terms of their direction cosines.

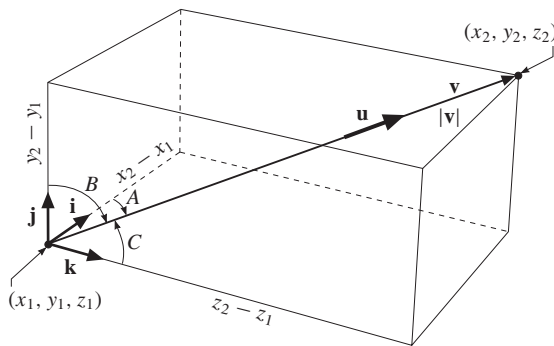


Figure 2.4

We now want to look at some examples to illustrate the use of direction angles, direction cosines, and unit vectors. Some of the diagrams that follow are printed in pairs with the righthand drawing rotated slightly to allow viewing in stereo. To view in stereo, relax the eyes to focus on a midpoint behind the diagrams—a third diagram in full stereo should now appear in the middle between the left and right ones. Some difficulty may be experienced at first: A method that might help is to put a sheet of glass over the diagram, then look for a faint image of your face behind the diagram. Focus your eyes on that image and then try to focus farther yet behind that image—the stereo image should now appear. It might not work at first, but daily attempts usually bring success. Of course, you must have fairly good vision out of both eyes, stereo perception with only one eye is not possible. However, the concept illustrated by the diagrams can still be obtained without the stereo effect.

**Example 2.2.1 Vector on the  $z$  axis.**

By inspection of Figure 2.5, we see that the direction angles of the vector  $\mathbf{v}$  are

$$A = 90 \text{ deg} \quad B = 90 \text{ deg} \quad C = 0 \text{ deg}$$

and so the direction cosines are

$$\alpha = 0 \quad \beta = 0 \quad \gamma = 1$$

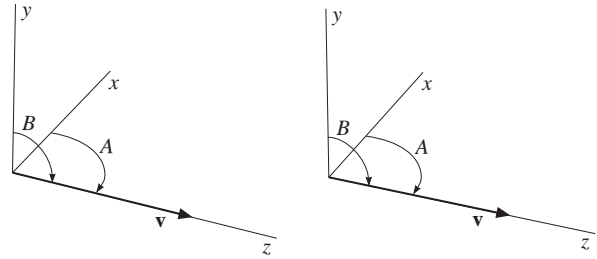


Figure 2.5

**Example 2.2.2 Vector on the  $-z$  axis.**

From Figure 2.6, we see that the direction angles are

$$A = 90 \text{ deg}, \quad B = 90 \text{ deg}, \quad C = 180 \text{ deg}$$

The corresponding direction cosines are

$$\alpha = 0, \quad \beta = 0, \quad \gamma = -1$$

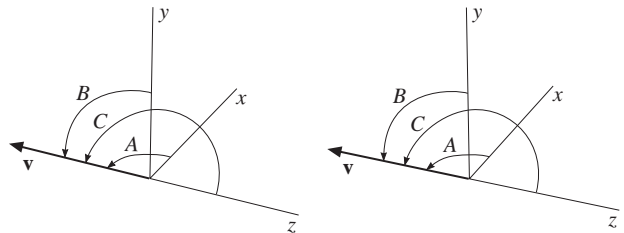


Figure 2.6

**Example 2.2.3 Vector not parallel to any of the axes.**

A vector that is not parallel to any of the axes and has its direction given by direction angles, or direction cosines, must be done carefully because only two of the three quantities are independent, as we discussed below the identity of Equation 2.4. Suppose we are given a vector  $\mathbf{v}$  of magnitude  $|\mathbf{v}| = 3$  units with the direction angles

$$A = 56.15 \text{ deg} \quad \text{and} \quad B = 137.97 \text{ deg}$$

To find the third direction angle  $C$ , we must use the identity of Equation 2.4, which requires knowledge of the the direction cosines. Thus,

$$\alpha = \cos A = 0.557021 \quad \text{and} \quad \beta = \cos B = -0.742794$$

We then calculate (we choose the  $+\sqrt{\quad}$  to get a forward-directed ray)

$$\gamma = +\sqrt{1 - \alpha^2 - \beta^2} = 0.371463$$

which corresponds to

$$C = \cos^{-1} \gamma = 68.19 \text{ deg}$$

The unit vector with these direction cosines is

$$\begin{aligned} \mathbf{u} &= \alpha \mathbf{i} + \beta \mathbf{j} + \gamma \mathbf{k} \\ &= 0.557021 \mathbf{i} - 0.742794 \mathbf{j} + 0.371463 \mathbf{k} \end{aligned}$$

and is parallel to the vector  $\mathbf{v}$ . Because we stated that the magnitude of  $\mathbf{v}$  was 3 units, we have

$$\mathbf{v} = 3\mathbf{u} = 1.67106 \mathbf{i} - 2.22838 \mathbf{j} + 1.11439 \mathbf{k}$$

The vectors  $\mathbf{v}$  and  $\mathbf{u}$  with their direction angles are graphed in Figure 2.7.

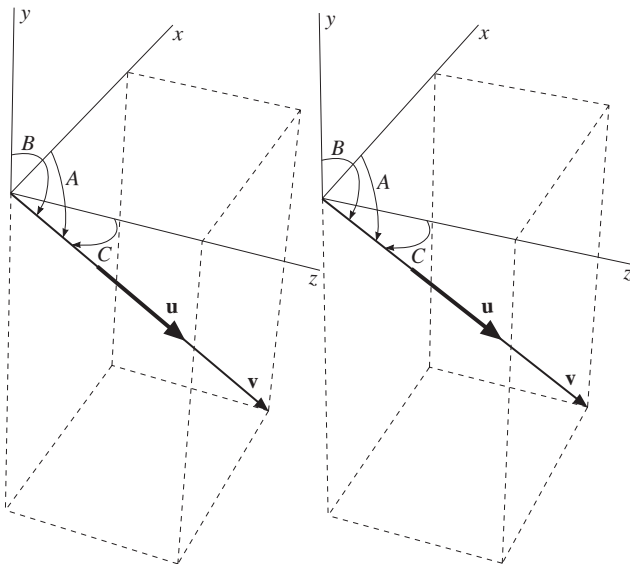


Figure 2.7

**Example 2.2.4 Vector given by its components.**

Suppose we are given the vector

$$\mathbf{v} = -2.00 \mathbf{i} + 3.00 \mathbf{j} + 3.50 \mathbf{k}$$

and we wish to find its direction cosines and direction angles, and then graph the vector. We first find the magnitude of the vector

$$v = |\mathbf{v}| = 5.02494$$

and then calculate the unit vector

$$\begin{aligned} \mathbf{u} &= \frac{\mathbf{v}}{|\mathbf{v}|} = \frac{-2.00 \mathbf{i} + 3.00 \mathbf{j} + 3.50 \mathbf{k}}{5.02494} \\ &= -0.398015 \mathbf{i} + 0.597022 \mathbf{j} + 0.696526 \mathbf{k} \end{aligned}$$

which is parallel to the vector  $\mathbf{v}$ , but has unit length—it is convenient to imagine that it lies somewhere on top of  $\mathbf{v}$ , as shown in Figure 2.8. The direction cosines are the components of  $\mathbf{u}$ ; thus,

$$\alpha = -0.398015, \quad \beta = 0.597022, \quad \gamma = 0.696526$$

and then the direction angles are

$$A = \cos^{-1} \alpha = 113.45 \text{ deg}$$

$$B = \cos^{-1} \beta = 53.34 \text{ deg}$$

$$C = \cos^{-1} \gamma = 45.85 \text{ deg}$$

These angles are shown in Figure 2.8.

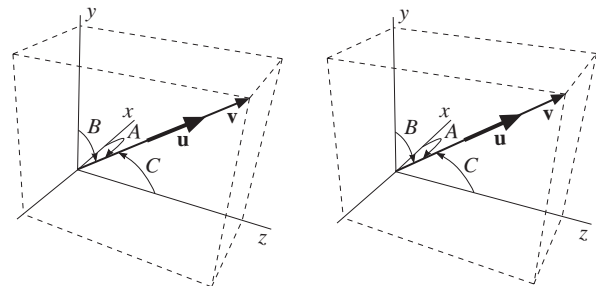


Figure 2.8

Again, we observe that the direction cosines satisfy the important identity of Equation 2.4, namely,

$$\begin{aligned} \alpha^2 + \beta^2 + \gamma^2 &= (-0.398015)^2 + (0.597022)^2 + (0.696526)^2 \\ &= 1 \end{aligned}$$

### 2.2.2 The dot product

The dot product is one way to multiply vectors. We give the polar-form definition of the product with the aid of Figure 2.9:

$$\begin{aligned} \mathbf{a} \cdot \mathbf{b} &= |\mathbf{a}| |\mathbf{b}| \cos \theta \\ &= a b \cos \theta \end{aligned} \quad (2.6)$$

where  $\theta$  is the smallest angle between the vectors with their tails touching—thus,  $0 \leq \theta \leq \pi$ ; also  $|\mathbf{a}| = a$  and  $|\mathbf{b}| = b$  are the magnitudes (or lengths) of the respective vectors. If the vector tails do not touch, then we move them parallel to their original directions until they do. We note that the dot product is a scalar; that is, a real number.

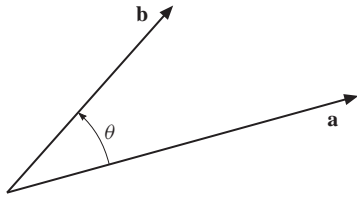


Figure 2.9 The dot product.

We use the polar form of the dot product to calculate nine values for the unit vectors  $\mathbf{i}, \mathbf{j}, \mathbf{k}$  with the help of Figure 2.10:

$$\left. \begin{array}{lll} \mathbf{i} \cdot \mathbf{i} = 1 & \mathbf{j} \cdot \mathbf{i} = 0 & \mathbf{k} \cdot \mathbf{i} = 0 \\ \mathbf{i} \cdot \mathbf{j} = 0 & \mathbf{j} \cdot \mathbf{j} = 1 & \mathbf{k} \cdot \mathbf{j} = 0 \\ \mathbf{i} \cdot \mathbf{k} = 0 & \mathbf{j} \cdot \mathbf{k} = 0 & \mathbf{k} \cdot \mathbf{k} = 1 \end{array} \right\} \quad (2.7)$$

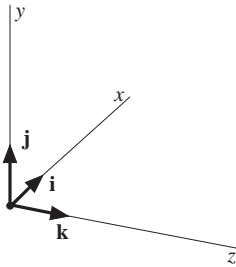


Figure 2.10

Then, when we have two vectors expressed in rectangular form as

$$\mathbf{a} = a_x \mathbf{i} + a_y \mathbf{j} + a_z \mathbf{k} \quad \text{and} \quad \mathbf{b} = b_x \mathbf{i} + b_y \mathbf{j} + b_z \mathbf{k}$$

we obtain the dot product in rectangular form by multiplying these expressions, and using Equation 2.7:

$$\begin{aligned} \mathbf{a} \cdot \mathbf{b} &= (a_x \mathbf{i} + a_y \mathbf{j} + a_z \mathbf{k}) \cdot (b_x \mathbf{i} + b_y \mathbf{j} + b_z \mathbf{k}) \\ &= a_x b_x \mathbf{i} \cdot \mathbf{i} + a_x b_y \mathbf{i} \cdot \mathbf{j} + a_x b_z \mathbf{i} \cdot \mathbf{k} \\ &\quad + a_y b_x \mathbf{j} \cdot \mathbf{i} + a_y b_y \mathbf{j} \cdot \mathbf{j} + a_y b_z \mathbf{j} \cdot \mathbf{k} \\ &\quad + a_z b_x \mathbf{k} \cdot \mathbf{i} + a_z b_y \mathbf{k} \cdot \mathbf{j} + a_z b_z \mathbf{k} \cdot \mathbf{k} \\ &= a_x b_x + a_y b_y + a_z b_z \end{aligned} \quad (2.8)$$

Both the polar and rectangular forms (see Equations 2.6 and 2.8) of the dot product are important: one form or the other, or both, may be required to solve a given problem.

Two identical vectors  $\mathbf{a}$  have an angle of  $\theta = 0$  between them; therefore, applying first the polar form, and then the rectangular form, gives

$$\mathbf{a} \cdot \mathbf{a} = a^2 = a_x^2 + a_y^2 + a_z^2 \quad (2.9)$$

We see that to square the magnitude of a vector, we calculate the dot product of a vector with itself. We also see that to get the magnitude  $|\mathbf{a}| = a$ , we simply take the square root.

Another use of the dot product is to pick out the direction cosines from the rectangular form expression of the unit vector  $\mathbf{u}$ :

$$\left. \begin{array}{l} \mathbf{u} \cdot \mathbf{i} = (\alpha \mathbf{i} + \beta \mathbf{j} + \gamma \mathbf{k}) \cdot \mathbf{i} \\ \quad = \alpha \mathbf{i} \cdot \mathbf{i} + \beta \mathbf{j} \cdot \mathbf{i} + \gamma \mathbf{k} \cdot \mathbf{i} = \alpha \\ \mathbf{u} \cdot \mathbf{j} = (\alpha \mathbf{i} + \beta \mathbf{j} + \gamma \mathbf{k}) \cdot \mathbf{j} \\ \quad = \alpha \mathbf{i} \cdot \mathbf{j} + \beta \mathbf{j} \cdot \mathbf{j} + \gamma \mathbf{k} \cdot \mathbf{j} = \beta \\ \mathbf{u} \cdot \mathbf{k} = (\alpha \mathbf{i} + \beta \mathbf{j} + \gamma \mathbf{k}) \cdot \mathbf{k} \\ \quad = \alpha \mathbf{i} \cdot \mathbf{k} + \beta \mathbf{j} \cdot \mathbf{k} + \gamma \mathbf{k} \cdot \mathbf{k} = \gamma \end{array} \right\} \quad (2.10)$$

The dot product is especially useful when we want to determine whether two vectors are perpendicular (or normal) to each other. Suppose we find that

$$\mathbf{a} \cdot \mathbf{b} = 0$$

Then the polar form of the dot product Equation 2.6 says that

$$a b \cos \theta = 0$$

and we must conclude that  $a = 0$  or  $b = 0$  or  $\cos \theta = 0$ . If neither  $a$  nor  $b$  are zero, we must have  $\cos \theta = 0$  which implies that  $\theta = \pi/2 \text{ rad} = 90 \text{ deg}$ ; that is,  $\mathbf{a}$  and  $\mathbf{b}$  are normal to each other.

On occasion, we must find the angle between two vectors; in three dimensions this calculation can be difficult. However, with the dot product, we can make this calculation quite easily, as the following example shows. Of course, this procedure works just as well in one or two dimensions.

---

#### Example 2.2.5 Calculation of the angle between two vectors in three dimensions.

Suppose it is given that

$$\mathbf{a} = -\mathbf{i} - \mathbf{j} - \mathbf{k} \quad \text{and} \quad \mathbf{b} = +\mathbf{i} + 2\mathbf{j} + 3\mathbf{k}$$

Using Equations 2.6, 2.8, and Equation 2.9, we obtain

$$\begin{aligned} \cos \theta &= \frac{\mathbf{a} \cdot \mathbf{b}}{a b} \\ &= \frac{a_x b_x + a_y b_y + a_z b_z}{\sqrt{a_x^2 + a_y^2 + a_z^2} \sqrt{b_x^2 + b_y^2 + b_z^2}} = -0.92582 \\ \theta &= 0.8766 \pi \text{ rad} = 157.8 \text{ deg} \end{aligned}$$


---

### 2.2.3 The cross product

Unlike the dot product, the cross product is a multiplication that produces a vector, not a scalar. But just like the dot product, the tails of the vectors are assumed to touch.

The polar form definition follows below with reference to Figure 2.11:

$$\begin{aligned}
 \mathbf{a} \times \mathbf{b} &= \text{a vector of} \\
 &\left. \begin{aligned}
 &1) \text{ magnitude } |\mathbf{a} \times \mathbf{b}| = ab \sin \theta, \text{ and} \\
 &2) \text{ direction perpendicular to both vectors } \mathbf{a} \\
 &\text{ and } \mathbf{b} \text{ with sense of direction given by the} \\
 &\text{ righthand rule: curl the fingers of the right} \\
 &\text{ hand such that they appear to push the first} \\
 &\text{ vector } \mathbf{a} \text{ into the second vector } \mathbf{b} \text{ through} \\
 &\text{ the smallest angle } \theta \text{ between them, and} \\
 &\text{ extend the thumb away from your fist—} \\
 &\text{ the extended thumb points in the direction} \\
 &\text{ of } \mathbf{a} \times \mathbf{b}.
 \end{aligned} \right\} (2.11)
 \end{aligned}$$

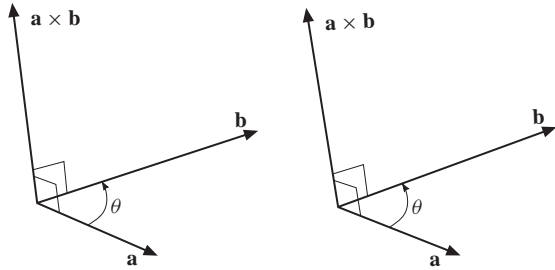


Figure 2.11 The cross product.

We use the polar form definition to obtain the cross product relations between the unit vectors:

$$\left. \begin{aligned}
 \mathbf{i} \times \mathbf{i} &= 0 & \mathbf{j} \times \mathbf{i} &= -\mathbf{k} & \mathbf{k} \times \mathbf{i} &= \mathbf{j} \\
 \mathbf{i} \times \mathbf{j} &= \mathbf{k} & \mathbf{j} \times \mathbf{j} &= 0 & \mathbf{k} \times \mathbf{j} &= -\mathbf{i} \\
 \mathbf{i} \times \mathbf{k} &= -\mathbf{j} & \mathbf{j} \times \mathbf{k} &= \mathbf{i} & \mathbf{k} \times \mathbf{k} &= 0
 \end{aligned} \right\} (2.12)$$

The memory circle shown in Figure 2.12 provides a quick way to recall these relations. For example, to find  $\mathbf{j} \times \mathbf{k}$ , read  $\mathbf{j}$  to  $\mathbf{k}$  on the memory circle and then keep going to the third vector  $\mathbf{i}$ ; since we move clockwise in the direction of the arrows, the result is positive, namely  $+\mathbf{i}$ . To find  $\mathbf{i} \times \mathbf{k}$ , the same procedure is followed, but since we move counterclockwise opposite to the arrow direction on the circle, the result is negative, namely  $-\mathbf{j}$ .

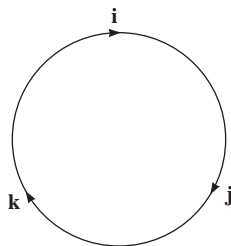


Figure 2.12 The memory circle.

Just as we derived the rectangular form for the dot product to obtain Equation 2.8, we start with two vectors given in rectangular form as

$$\mathbf{a} = a_x \mathbf{i} + a_y \mathbf{j} + a_z \mathbf{k} \quad \text{and} \quad \mathbf{b} = b_x \mathbf{i} + b_y \mathbf{j} + b_z \mathbf{k}$$

then multiply them together, and use Equation 2.12 to simplify the unit vector cross products:

$$\begin{aligned}
 \mathbf{a} \times \mathbf{b} &= (a_x \mathbf{i} + a_y \mathbf{j} + a_z \mathbf{k}) \times (b_x \mathbf{i} + b_y \mathbf{j} + b_z \mathbf{k}) \\
 &= a_x b_x \mathbf{i} \times \mathbf{i} + a_x b_y \mathbf{i} \times \mathbf{j} + a_x b_z \mathbf{i} \times \mathbf{k} \\
 &\quad + a_y b_x \mathbf{j} \times \mathbf{i} + a_y b_y \mathbf{j} \times \mathbf{j} + a_y b_z \mathbf{j} \times \mathbf{k} \\
 &\quad + a_z b_x \mathbf{k} \times \mathbf{i} + a_z b_y \mathbf{k} \times \mathbf{j} + a_z b_z \mathbf{k} \times \mathbf{k} \\
 &= \mathbf{i}(a_y b_z - a_z b_y) \\
 &\quad - \mathbf{j}(a_x b_z - a_z b_x) \\
 &\quad + \mathbf{k}(a_x b_y - a_y b_x) \\
 &= \begin{vmatrix} \mathbf{i} & \mathbf{j} & \mathbf{k} \\ a_x & a_y & a_z \\ b_x & b_y & b_z \end{vmatrix} \quad (2.13)
 \end{aligned}$$

The determinant in the last step of this equation is not an ordinary one, since the elements in the first row are vectors, not scalars. However, if we expand the determinant according to the usual rules, we more easily obtain the correct expression for the rectangular form of the cross product, which appears above the determinant in Equation 2.13.

It is important to note that the polar form of the cross product quickly predicts

$$\mathbf{a} \times \mathbf{a} = 0$$

because the angle between two identical vectors is zero.

One of the interesting properties of the cross product is that it does not obey the commutative law; that is,  $\mathbf{a} \times \mathbf{b}$  is not equal to  $\mathbf{b} \times \mathbf{a}$ . Instead, the cross product obeys the anticommutative law, namely

$$\mathbf{a} \times \mathbf{b} = -\mathbf{b} \times \mathbf{a}$$

which follows from the polar form definition, Equation 2.11.

The equation that is the analog of  $\mathbf{a} \cdot \mathbf{b} = 0$  is

$$\mathbf{a} \times \mathbf{b} = 0$$

Then Equation 2.11 implies

$$|\mathbf{a} \times \mathbf{b}| = ab \sin \theta = 0$$

which says that either  $a = 0$  or  $b = 0$  or  $\sin \theta = 0$ . If neither  $a = 0$  nor  $b = 0$ , then  $\sin \theta = 0$ , and we conclude that  $\theta = 0$  or  $\theta = \pi \text{ rad} = 180 \text{ deg}$ ; that is,  $\mathbf{a}$  is parallel/antiparallel to  $\mathbf{b}$ . Thus, with the dot product we can determine when two vectors are normal to each other; with the cross product, when two vectors are parallel/antiparallel.

### 2.3 Exact Ray Tracing of Skew Rays

The most general ray is a skew ray, and includes as a special case, the paraxial ray. Its direction is conveniently described by the direction angles  $A, B, C$  and the direction cosines  $\alpha, \beta, \gamma$  which we discussed in the Section 2.2.1. In this section we derive equations without approximations that describe the behavior of a skew ray as it translates from one point to another located on a spherical surface, and then is refracted at the surface. Because skew rays travel in three dimensions, it is not easy to obtain equations which describe their translation and refraction properties by simple inspection of a diagram. Thus, we use vector methods which are a great aid in work of three dimensions. Especially advantageous is the unit vector  $\mathbf{u}$  because its components are the direction cosines of a ray. To simplify the algebraic notation in the derivations, we shall minimize the use of subscripts.

#### 2.3.1 The translation equations

In Figure 2.13, we show a skew ray that travels from a point  $P$  to a point  $P_1$  on a spherical surface of radius  $r$ , center of curvature  $C$ , and with the vertex  $V$  where it intersects the  $z$  axis. The point  $P$  is the starting point of the ray, which can be a point on another spherical surface where the ray was

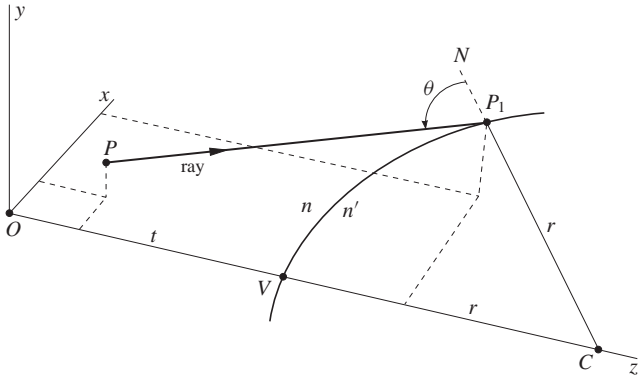


Figure 2.13

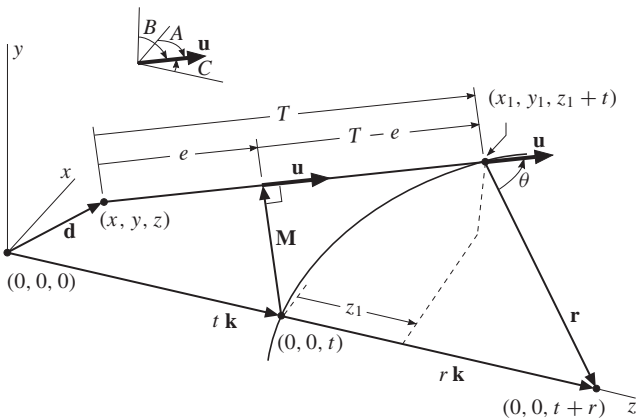


Figure 2.14

refracted. The radius  $r$  that intersects the surface at  $P_1$ , and is then extended, is also the normal  $N$  to the surface. The angle  $\theta$  between  $N$  and the ray is the angle of incidence.

We now redraw Figure 2.13 as Figure 2.14 with the vectors in place to help in the derivation of the equations. By invoking the rule of geometry that opposite angles are equal, we move  $\theta$  in Figure 2.13 to the location between the vectors  $\mathbf{u}$  and  $\mathbf{r}$  in Figure 2.14. We write in the coordinates of some of the points to make it easier to express several of the vectors. Note that the coordinates  $(x_1, y_1, z_1 + t)$  of point  $P_1$  have the  $z$  coordinate expressed as  $z_1 + t$ ; that is,  $z_1$  is measured from the vertex  $V$  of the spherical surface. This method is used throughout the ray tracing procedure to keep the  $z$  coordinates of roughly the same numerical size as the  $x, y$  coordinates, and thus avoid large-number/small-number problems which might occur as the ray is traced through the optical system.

Our goal is to obtain equations so that we can calculate values for the ray translation  $T$ ,  $\cos \theta$ , and the coordinates  $(x_1, y_1, z_1)$  of the point  $P_1$  on the refracting surface. Given quantities are the coordinates of the point  $P$ , namely  $(x, y, z)$ , the distance  $t$  along the  $z$  axis from the origin  $O$  to the vertex  $V$ , the radius  $r$ —a positive quantity for the convex surface shown in the diagrams—and the direction of ray travel given by the direction angles  $A, B, C$  (see insert in Figure 2.14), or the direction cosines  $\alpha, \beta, \gamma$  of the unit vector  $\mathbf{u}$ . We have

$$\mathbf{u} = \alpha \mathbf{i} + \beta \mathbf{j} + \gamma \mathbf{k} \tag{2.14}$$

where

$$\alpha = \cos A, \quad \beta = \cos B, \quad \gamma = \cos C \tag{2.15}$$

We start the equation derivation by first writing two vector expressions by inspection of Figure 2.14:

$$\mathbf{d} = x \mathbf{i} + y \mathbf{j} + z \mathbf{k} \tag{2.16}$$

and

$$\begin{aligned} \mathbf{r} &= (0 - x_1) \mathbf{i} + (0 - y_1) \mathbf{j} + (t + r - z_1 - t) \mathbf{k} \\ &= -x_1 \mathbf{i} - y_1 \mathbf{j} - (z_1 - r) \mathbf{k} \end{aligned} \tag{2.17}$$

Then we apply the vector addition concept to several of the vectors shown in the diagram, namely

$$\mathbf{d} + T \mathbf{u} + \mathbf{r} = (t + r) \mathbf{k} \tag{2.18}$$

Substituting Equations 2.14, 2.16, 2.17 into Equation 2.18 and rearranging, we obtain

$$\begin{aligned} (x_1 - x - T\alpha) \mathbf{i} \\ + (y_1 - y - T\beta) \mathbf{j} \\ + (z_1 - z - T\gamma + t) \mathbf{k} = 0 \end{aligned} \tag{2.19}$$



A vector is zero only when each of its components is zero; therefore, each of the component expressions—the coefficients of the  $\mathbf{i}$ ,  $\mathbf{j}$ ,  $\mathbf{k}$ —in Equation 2.19 must equal zero. Thus, we have

$$x_1 = x + T\alpha \quad (2.20a)$$

$$y_1 = y + T\beta \quad (2.20b)$$

$$z_1 = z + T\gamma - t \quad (2.20c)$$

where we have set each of component expressions to zero, and then solved for  $x_1$ ,  $y_1$ ,  $z_1$  respectively. All the quantities in Equations 2.20 are known except  $T$ ; to obtain an equation for this quantity is more difficult.

The vector  $\mathbf{M}$  in Figure 2.14 is drawn normal to the unit vector  $\mathbf{u}$ ;  $\mathbf{M}$  is used as an aid to obtain the equations we need. By inspection of Figure 2.14, we get the vector equation

$$\mathbf{d} + e\mathbf{u} = t\mathbf{k} + \mathbf{M} \quad (2.21)$$

where the meaning of  $e$  is shown in Figure 2.14. To obtain an expression for  $e$  in terms of known quantities, we solve Equation 2.21 for  $e\mathbf{u}$ :

$$e\mathbf{u} = t\mathbf{k} - \mathbf{d} + \mathbf{M}$$

To obtain  $e$  alone, we dot multiply both sides of this equation by the unit vector  $\mathbf{u}$ :

$$e\mathbf{u} \cdot \mathbf{u} = t\mathbf{k} \cdot \mathbf{u} - \mathbf{d} \cdot \mathbf{u} + \mathbf{M} \cdot \mathbf{u}$$

Because  $\mathbf{u}$  is a unit vector,  $\mathbf{u} \cdot \mathbf{u} = 1$ , and because  $\mathbf{M}$  is normal to  $\mathbf{u}$ , we have  $\mathbf{M} \cdot \mathbf{u} = 0$ ; therefore, our equation simplifies to

$$e = t\mathbf{k} \cdot \mathbf{u} - \mathbf{d} \cdot \mathbf{u}$$

Finally, we substitute Equations 2.14 and 2.16, and dot multiply, to get

$$\begin{aligned} e &= t\mathbf{k} \cdot (\alpha\mathbf{i} + \beta\mathbf{j} + \gamma\mathbf{k}) \\ &\quad - (x\mathbf{i} + y\mathbf{j} + z\mathbf{k}) \cdot (\alpha\mathbf{i} + \beta\mathbf{j} + \gamma\mathbf{k}) \\ &= t\gamma - (x\alpha + y\beta + z\gamma) \end{aligned} \quad (2.22)$$

and we have obtained  $e$  in terms of known quantities.

To acquire the next useful result, we first solve Equation 2.21 for  $\mathbf{M}$  to get

$$\mathbf{M} = \mathbf{d} + e\mathbf{u} - t\mathbf{k} \quad (2.23)$$

and then dot multiply both sides of this equation by  $\mathbf{k}$ :

$$\mathbf{M} \cdot \mathbf{k} = \mathbf{d} \cdot \mathbf{k} + e\mathbf{u} \cdot \mathbf{k} - t\mathbf{k} \cdot \mathbf{k}$$

In this equation,  $\mathbf{M} \cdot \mathbf{k} = M_z$  and  $\mathbf{k} \cdot \mathbf{k} = 1$ ; therefore, we can simplify the equation to

$$M_z = \mathbf{d} \cdot \mathbf{k} + e\mathbf{u} \cdot \mathbf{k} - t$$

Just as in the final step to get Equation 2.22, we substitute Equations 2.14 and 2.16, and dot multiply, to obtain

$$\begin{aligned} M_z &= (x\mathbf{i} + y\mathbf{j} + z\mathbf{k}) \cdot \mathbf{k} \\ &\quad + e(\alpha\mathbf{i} + \beta\mathbf{j} + \gamma\mathbf{k}) \cdot \mathbf{k} - t \\ &= z + e\gamma - t \end{aligned} \quad (2.24)$$

and we have  $M_z$ , the  $z$  component of  $\mathbf{M}$ , in terms of given or calculated quantities.

Again we start with Equation 2.21, but solve it for  $\mathbf{d} - t\mathbf{k}$  to obtain

$$\mathbf{d} - t\mathbf{k} = \mathbf{M} - e\mathbf{u}$$

which we dot multiply on both sides by  $\mathbf{u}$ :

$$\begin{aligned} (\mathbf{d} - t\mathbf{k}) \cdot \mathbf{u} &= (\mathbf{M} - e\mathbf{u}) \cdot \mathbf{u} \\ &= \mathbf{M} \cdot \mathbf{u} - e\mathbf{u} \cdot \mathbf{u} \\ &= 0 - e \\ &= -e \end{aligned} \quad (2.25)$$

We put this equation on hold for later use in Equation 2.28b. Going back to Equation 2.21, and solving for  $\mathbf{M}$ :

$$\begin{aligned} \mathbf{M} &= \mathbf{d} + e\mathbf{u} - t\mathbf{k} \\ &= (\mathbf{d} - t\mathbf{k}) + e\mathbf{u} \end{aligned} \quad (2.26)$$

We square both sides of Equation 2.26 by using the dot product operation:

$$\begin{aligned} \mathbf{M} \cdot \mathbf{M} &= [(\mathbf{d} - t\mathbf{k}) + e\mathbf{u}] \cdot [(\mathbf{d} - t\mathbf{k}) + e\mathbf{u}] \\ M^2 &= (\mathbf{d} - t\mathbf{k}) \cdot (\mathbf{d} - t\mathbf{k}) \\ &\quad + 2(\mathbf{d} - t\mathbf{k}) \cdot e\mathbf{u} + e\mathbf{u} \cdot e\mathbf{u} \end{aligned} \quad (2.27)$$

Working with the terms on the right side of Equation 2.27, we expand the first term to obtain

$$\begin{aligned} (\mathbf{d} - t\mathbf{k}) \cdot (\mathbf{d} - t\mathbf{k}) &= \mathbf{d} \cdot \mathbf{d} - 2t\mathbf{k} \cdot \mathbf{d} + t\mathbf{k} \cdot t\mathbf{k} \\ &= (x\mathbf{i} + y\mathbf{j} + z\mathbf{k}) \cdot (x\mathbf{i} + y\mathbf{j} + z\mathbf{k}) \\ &\quad - 2t\mathbf{k} \cdot (x\mathbf{i} + y\mathbf{j} + z\mathbf{k}) + t^2\mathbf{k} \cdot \mathbf{k} \\ &= x^2 + y^2 + z^2 - 2tz + t^2 \end{aligned} \quad (2.28a)$$

where we have substituted Equation 2.16 for  $\mathbf{d}$ . In the second term of Equation 2.27, we substitute Equation 2.25 in the middle expression below:

$$2(\mathbf{d} - t\mathbf{k}) \cdot e\mathbf{u} = 2e(\mathbf{d} - t\mathbf{k}) \cdot \mathbf{u} = -2e^2 \quad (2.28b)$$

For the third term, we quickly obtain

$$e\mathbf{u} \cdot e\mathbf{u} = e^2 \quad (2.28c)$$

Substituting Equations 2.28 into Equation 2.27, we have  $M^2$  described with known quantities:

$$\begin{aligned} M^2 &= x^2 + y^2 + z^2 - 2tz + t^2 - 2e^2 + e^2 \\ &= x^2 + y^2 + z^2 - e^2 + t^2 - 2tz \end{aligned} \quad (2.29)$$

where we have simplified and rearranged terms slightly in the last expression.

Another vector equation by inspection of Figure 2.14 is

$$\mathbf{M} + (T - e)\mathbf{u} + \mathbf{r} = r\mathbf{k} \quad (2.30)$$

or

$$(T - e)\mathbf{u} = r\mathbf{k} - \mathbf{M} - \mathbf{r} \quad (2.31)$$

Then dot multiplying both sides of this equation by  $\mathbf{u}$ , we write the equations

$$\begin{aligned} (T - e)\mathbf{u} \cdot \mathbf{u} &= r\mathbf{k} \cdot \mathbf{u} - \mathbf{M} \cdot \mathbf{u} - \mathbf{r} \cdot \mathbf{u} \\ T - e &= r\gamma - 0 - \mathbf{r} \cdot \mathbf{u} \\ &= r\gamma - |\mathbf{r}| |\mathbf{u}| \cos \theta \\ &= r\gamma - r \cos \theta \\ &= \frac{\gamma - \cos \theta}{c} \end{aligned} \quad (2.32)$$

where  $c = 1/r$  is the curvature. We have used the polar form of the dot product to evaluate  $\mathbf{r} \cdot \mathbf{u}$  to bring in the angle of incidence  $\theta$ .

However, there are two unknowns in Equation 2.32:  $T$  and  $\cos \theta$ . To obtain separate expressions for these two unknowns, we take Equation 2.30 and solve it for  $\mathbf{M} - r\mathbf{k}$ ; thus,

$$\mathbf{M} - r\mathbf{k} = -[(T - e)\mathbf{u} + \mathbf{r}] \quad (2.33)$$

Next, we square both sides of this equation by using the dot product:

$$(\mathbf{M} - r\mathbf{k}) \cdot (\mathbf{M} - r\mathbf{k}) = [(T - e)\mathbf{u} + \mathbf{r}] \cdot [(T - e)\mathbf{u} + \mathbf{r}]$$

where the minus sign in front of the brackets in Equation 2.33 has disappeared in the squaring operation. We expand the dot products to get

$$\begin{aligned} \mathbf{M} \cdot \mathbf{M} - 2r\mathbf{M} \cdot \mathbf{k} + r^2\mathbf{k} \cdot \mathbf{k} \\ &= (T - e)^2\mathbf{u} \cdot \mathbf{u} + 2(T - e)\mathbf{r} \cdot \mathbf{u} + \mathbf{r} \cdot \mathbf{r} \\ M^2 - 2rM_z + r^2 \\ &= (T - e)^2 + 2(T - e)r \cos \theta + r^2 \end{aligned} \quad (2.34)$$

We cancel the  $r^2$  terms in Equation 2.34, replace the remaining  $r$  terms by  $1/c$ , substitute for  $T - e$  with Equation 2.32, and solve for  $\cos \theta$  to obtain after some manipulation

$$\cos \theta = +\sqrt{\gamma^2 - c(cM^2 - 2M_z)} \quad (2.35)$$

where we choose the positive square root because  $\cos \theta$  is positive for an angle of incidence.

Because we now know  $\cos \theta$  from Equation 2.35, we can calculate  $T$  from Equation 2.32 as

$$T = e + \frac{\gamma - \cos \theta}{c} \quad (2.36)$$

However, this equation has an unfortunate property when the surface is plane for then  $c = 0$  and we have a divide by zero. We put this equation into a better form as follows:

$$\begin{aligned} T &= e + \frac{\gamma - \cos \theta}{c} \left( \frac{\gamma + \cos \theta}{\gamma + \cos \theta} \right) \\ &= e + \frac{\gamma^2 - \cos^2 \theta}{c(\gamma + \cos \theta)} \end{aligned}$$

Substituting Equation 2.35 for the  $\cos^2 \theta$  in the numerator, we obtain after simplification

$$T = e + \frac{cM^2 - 2M_z}{\gamma + \cos \theta} \quad (2.37)$$

and we have achieved our goal: we no longer divide by zero when  $c$  is zero. Both Equations 2.35 and 2.37 have righthand sides composed of given or calculated quantities.

With knowledge of  $T$  from Equation 2.37, we can substitute into Equations 2.20 and determine  $x_1, y_1, z_1$ , which form the point  $P_1$  where the ray intersects the surface (see Figures 2.13 and 2.14). Because  $x_1, y_1, z_1$  are on a spherical surface, they must satisfy the equation of a sphere, namely

$$x_1^2 + y_1^2 + (z_1 - r)^2 = r^2$$

or

$$x_1^2 + y_1^2 + z_1^2 - 2rz_1 = 0 \quad (2.38)$$

As Figures 2.13 and 2.14 show, this sphere has its center on the  $z$  axis at  $C$ , and the origin is at  $V$ .

We will summarize the important equations derived in this section later in a flow chart (see Figure 2.19).

**A closer look at  $\mathbf{r} \cdot \mathbf{u} = |\mathbf{r}| |\mathbf{u}| \cos \theta$ .** There is a problem in evaluating  $|\mathbf{r}|$  in the dot product  $\mathbf{r} \cdot \mathbf{u} = |\mathbf{r}| |\mathbf{u}| \cos \theta$ . By definition,  $|\mathbf{r}|$ , the magnitude of  $\mathbf{r}$ , is always positive. But in optics,  $r$  is positive for convex surfaces, negative for concave surfaces. So when we say  $|\mathbf{r}| = r$ , as we did when we derived Equation 2.32, we have a problem when the surface is concave—for when the surface is concave, the rules of vector algebra say that we should write  $|\mathbf{r}| = -r$  (because  $r < 0$  for concave surfaces).

To attack this problem, we go back to the derivation of Equation 2.32, solve the equation for  $T$  with the  $\mathbf{r} \cdot \mathbf{u}$  term, and then rewrite the equation correctly for both a convex and concave surface:

$$\begin{aligned} T &= e + r\gamma - \mathbf{r} \cdot \mathbf{u} \\ &= e + r\gamma - \begin{bmatrix} +r \cos \theta \\ -r \cos \theta'' \end{bmatrix} \end{aligned} \quad (2.39)$$

where inside the brackets on the top line we have written  $|\mathbf{r}| = +r$  for a convex surface, and on the bottom line we have  $|\mathbf{r}| = -r$  for a concave surface (remember,  $|\mathbf{r}|$  must equal a positive number, and  $-r > 0$  because  $r < 0$  for a concave surface). Also in Equation 2.39, we have written  $\theta$  for the angle between  $\mathbf{r}$  and  $\mathbf{u}$  when the surface is convex, and  $\theta''$  when it is a concave surface, as we indicate in Figure 2.15. The  $r\gamma$  term in Equation 2.39 does not cause a problem,  $r$  is simply replaced by a positive or negative value for a convex or concave surface, respectively.

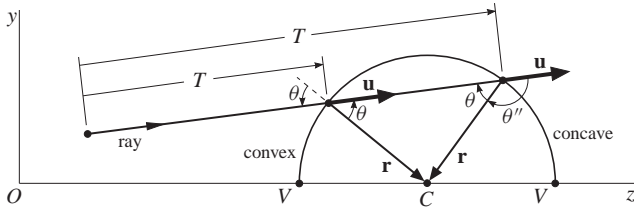


Figure 2.15

In Figure 2.15, we have drawn a semicircle so that the left side represents a convex surface, and the right side a concave surface. We also assume that the semicircle represents a spherical surface that encloses a medium that is the same as the medium outside, say air, to eliminate the need to worry about refraction. To make it easier, we have drawn the diagram in the  $yz$  plane; however, it works in three dimensions just as well. First of all, we see that there is no problem with the convex surface for  $\theta$  is the angle of incidence as well as the angle between  $\mathbf{r}$  and  $\mathbf{u}$ . However, for the concave surface,  $\theta$  is the angle of incidence, and  $\theta''$  is the angle between  $\mathbf{r}$  and  $\mathbf{u}$ . Because  $\theta'' = \pi - \theta$ , we have

$$\cos \theta'' = \cos(\pi - \theta) = -\cos \theta \quad (2.40)$$

Substituting Equation 2.40 into Equation 2.39 gives

$$\begin{aligned} T &= e + r\gamma - \begin{bmatrix} +r \cos \theta \\ -r \cos \theta'' \end{bmatrix} \\ &= e + r\gamma - \begin{bmatrix} +r \cos \theta \\ +r \cos \theta \end{bmatrix} \\ &= e + r\gamma - r \cos \theta \end{aligned} \quad (2.41)$$

Thus, Equation 2.41 is the same for either a convex or concave surface when we use the angle of incidence  $\theta$ , which is perfect for our purposes—all we have to do is remember that  $r$  equals a positive number for a convex surface and a negative number for a concave surface. In conclusion, the translation equations that we have derived are correct for both convex and concave surfaces.

One last observation in Figure 2.15 is that  $T$  is greater for a concave surface, consistent with  $(-r \cos \theta) > 0$ ; it is smaller for a convex surface, which is compatible with  $(-r \cos \theta) < 0$ .

### 2.3.2 The refraction equations

The diagram in Figure 2.16 shows refraction at the point  $P_1$  for a skew ray. The normal to the refracting surface is  $N$ , the angle of incidence is  $\theta$ , and the angle of refraction is  $\theta'$ . The vector  $\mathbf{r}$  is the radius vector and has magnitude  $|\mathbf{r}| = r$ , which is the radius of the surface (positive for the convex surface shown in the diagram)—this vector, along with its backward extension, forms the normal  $N$  to the surface. The unit vector  $\mathbf{u}$  with its direction cosines  $\alpha, \beta, \gamma$  gives the direction of the incident ray; the corresponding unit vector  $\mathbf{u}'$  with its direction cosines  $\alpha', \beta', \gamma'$  gives the direction of the refracted ray. The vectors  $\mathbf{u}, \mathbf{r}, \mathbf{u}'$  form the plane of incidence; remember, the incident ray, the normal, and the refracted ray lie in this plane (as required by the law of refraction). As usual,  $n$  is the index of refraction to the left of the surface,  $n'$  to the right of the surface.

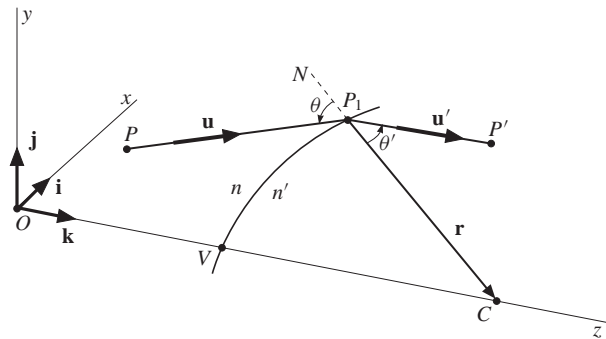


Figure 2.16

In this section, we want to obtain  $\alpha', \beta', \gamma'$  in terms of given or previously calculated quantities. Our first step toward this goal is to draw Figure 2.17, and use it as a guide

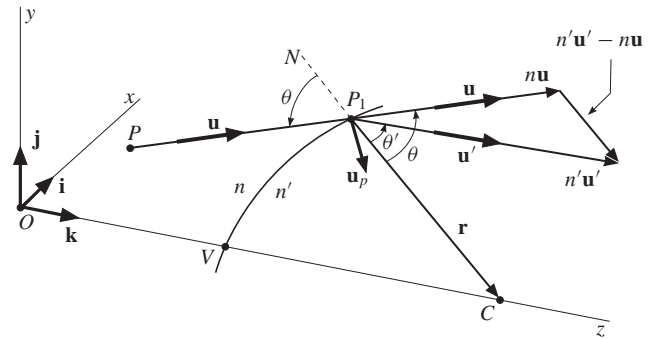


Figure 2.17

to prove that  $n'\mathbf{u}' - n\mathbf{u}$  is parallel/antiparallel to the radius vector  $\mathbf{r}$ . In this diagram,  $\mathbf{u}_p$  is a unit vector normal (or perpendicular) to the plane of incidence; that is, it is normal to the vectors  $\mathbf{u}, \mathbf{r}, \mathbf{u}'$ . We construct the proof with the polar form of the cross product (see Equation 2.11):

$$\begin{aligned} (n'\mathbf{u}' - n\mathbf{u}) \times \mathbf{r} &= n'\mathbf{u}' \times \mathbf{r} - n\mathbf{u} \times \mathbf{r} \\ &= n'(1)r \sin \theta' \mathbf{u}_p - n(1)r \sin \theta \mathbf{u}_p \\ &= r(n' \sin \theta' - n \sin \theta) \mathbf{u}_p \\ &= 0 \end{aligned} \quad (2.42)$$

and obtain the zero in the last step using Equation 1.2, the law of refraction:  $n \sin \theta = n' \sin \theta'$ .

Because the cross product between the vectors  $n' \mathbf{u}' - n \mathbf{u}$  and  $\mathbf{r}$  is zero, these vectors must be parallel or antiparallel to each other by the conclusion we drew at the end of Section 2.2.3 on the cross product. In other words, the vector  $n' \mathbf{u}' - n \mathbf{u}$  points in the same or opposite direction to  $\mathbf{r}$ , only its magnitude may differ from that of  $\mathbf{r}$ . Therefore, these two vectors must be related to each other by a scalar; that is, by some real number (positive or negative) that we shall call  $G$ :

$$n' \mathbf{u}' - n \mathbf{u} = G \mathbf{r} \quad (2.43a)$$

To get an expression for  $G$ , we dot multiply both sides of Equation 2.43a by  $\mathbf{r}$  to obtain

$$\begin{aligned} (n' \mathbf{u}' - n \mathbf{u}) \cdot \mathbf{r} &= G \mathbf{r} \cdot \mathbf{r} \\ n' \mathbf{u}' \cdot \mathbf{r} - n \mathbf{u} \cdot \mathbf{r} &= G r^2 \end{aligned} \quad (2.43b)$$

Inspecting Figure 2.17, we see that the polar form of the dot product gives (works also when  $r < 0$ , see Problem 2.17)

$$\mathbf{u}' \cdot \mathbf{r} = r \cos \theta' \quad \text{and} \quad \mathbf{u} \cdot \mathbf{r} = r \cos \theta \quad (2.43c)$$

Substituting the expressions in Equation 2.43c into Equation 2.43b, interchanging the left and right sides, we get

$$\begin{aligned} G r^2 &= n' r \cos \theta' - n r \cos \theta \\ G &= \frac{n' \cos \theta' - n \cos \theta}{r} \\ &= c(n' \cos \theta' - n \cos \theta) \\ &= cn' \left( \cos \theta' - \frac{n}{n'} \cos \theta \right) \\ &= cn' (\cos \theta' - \mu \cos \theta) \\ &= cn' g \end{aligned} \quad (2.44)$$

where we have replaced  $r$  by  $1/c$ , and where

$$\mu = \frac{n}{n'} \quad (2.45)$$

and

$$g = \cos \theta' - \mu \cos \theta \quad (2.46)$$

We can calculate  $\cos \theta$  from Equation 2.35, but we have no equation yet for  $\cos \theta'$ . To obtain this latter equation we start with the law of refraction, and then use a trig identity:

$$\begin{aligned} n \sin \theta &= n' \sin \theta' \\ \sin \theta' &= \frac{n}{n'} \sin \theta \\ \sqrt{1 - \cos^2 \theta'} &= \frac{n}{n'} \sqrt{1 - \cos^2 \theta} \end{aligned}$$

We now square both sides of previous equation, substitute Equation 2.45, and solve for  $\cos \theta'$ :

$$\begin{aligned} 1 - \cos^2 \theta' &= \mu^2 (1 - \cos^2 \theta) \\ \cos^2 \theta' &= 1 - \mu^2 (1 - \cos^2 \theta) \\ \cos \theta' &= +\sqrt{1 - \mu^2 (1 - \cos^2 \theta)} \end{aligned} \quad (2.47)$$

We have now obtained the necessary equations to calculate  $g$  as given in Equation 2.46.

Finally, we want the direction cosines  $\alpha'$ ,  $\beta'$ ,  $\gamma'$ —which give the direction angles  $A'$ ,  $B'$ ,  $C'$ —for the refracted ray. This information is represented by the respective unit vectors for the incident and refracted rays, as illustrated in Figure 2.18, and written as

$$\begin{aligned} \mathbf{u} &= \cos A \mathbf{i} + \cos B \mathbf{j} + \cos C \mathbf{k} \\ &= \alpha \mathbf{i} + \beta \mathbf{j} + \gamma \mathbf{k} \end{aligned} \quad (2.48)$$

and

$$\begin{aligned} \mathbf{u}' &= \cos A' \mathbf{i} + \cos B' \mathbf{j} + \cos C' \mathbf{k} \\ &= \alpha' \mathbf{i} + \beta' \mathbf{j} + \gamma' \mathbf{k} \end{aligned} \quad (2.49)$$

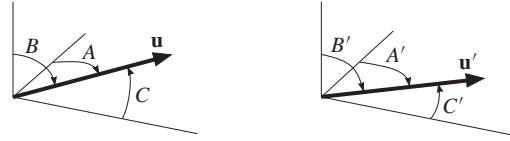


Figure 2.18

We start with Equation 2.43a using Equation 2.44 to replace  $G$ :

$$n' \mathbf{u}' - n \mathbf{u} = cn' g \mathbf{r} \quad (2.50)$$

and then substitute Equation 2.17 for  $\mathbf{r}$  to get

$$n' \mathbf{u}' - n \mathbf{u} = cn' g [-x_1 \mathbf{i} - y_1 \mathbf{j} - (z_1 - r) \mathbf{k}] \quad (2.51)$$

We find  $\alpha'$  by dot multiplying both sides of Equation 2.51 by  $\mathbf{i}$ , as follows:

$$\begin{aligned} n' \underbrace{\mathbf{u}' \cdot \mathbf{i}}_{\alpha'} - n \underbrace{\mathbf{u} \cdot \mathbf{i}}_{\alpha} &= cn' g [-x_1 \underbrace{\mathbf{i} \cdot \mathbf{i}}_1 - y_1 \underbrace{\mathbf{j} \cdot \mathbf{i}}_0 - (z_1 - r) \underbrace{\mathbf{k} \cdot \mathbf{i}}_0] \\ n' \alpha' - n \alpha &= -cn' g x_1 \\ \alpha' &= \mu \alpha - cg x_1 \end{aligned} \quad (2.52a)$$

Similarly, we find  $\beta'$  by dot multiplying both sides of Equation 2.51 by  $\mathbf{j}$ :

$$\beta' = \mu \beta - cg y_1 \quad (2.52b)$$

Lastly, we obtain  $\gamma'$  by multiplying both sides of Equation 2.51 by  $\mathbf{k}$ —the result has an extra term because  $z_1$  is measured from the vertex  $V$  (see Figures 2.13 and 2.14):

$$\gamma' = \mu \gamma - cg z_1 + g \quad (2.52c)$$

where we replaced the  $r$  in  $(z_1 - r)$  of Equation 2.51 by  $1/c$ .

Based on Equation 2.4, the primed direction cosines satisfy

$$\alpha'^2 + \beta'^2 + \gamma'^2 = 1 \quad (2.53)$$

### 2.3.3 Summary of equations and application

We have now finished the derivation of all the translation and refraction equations for exact ray tracing. One of the attractive features of these equations is that they work for all spherical surfaces: convex ( $r$  or  $c > 0$ ), concave ( $r$  or  $c < 0$ ), and plane ( $r = \infty$  or  $c = 0$ ). The flow chart in Figure 2.19

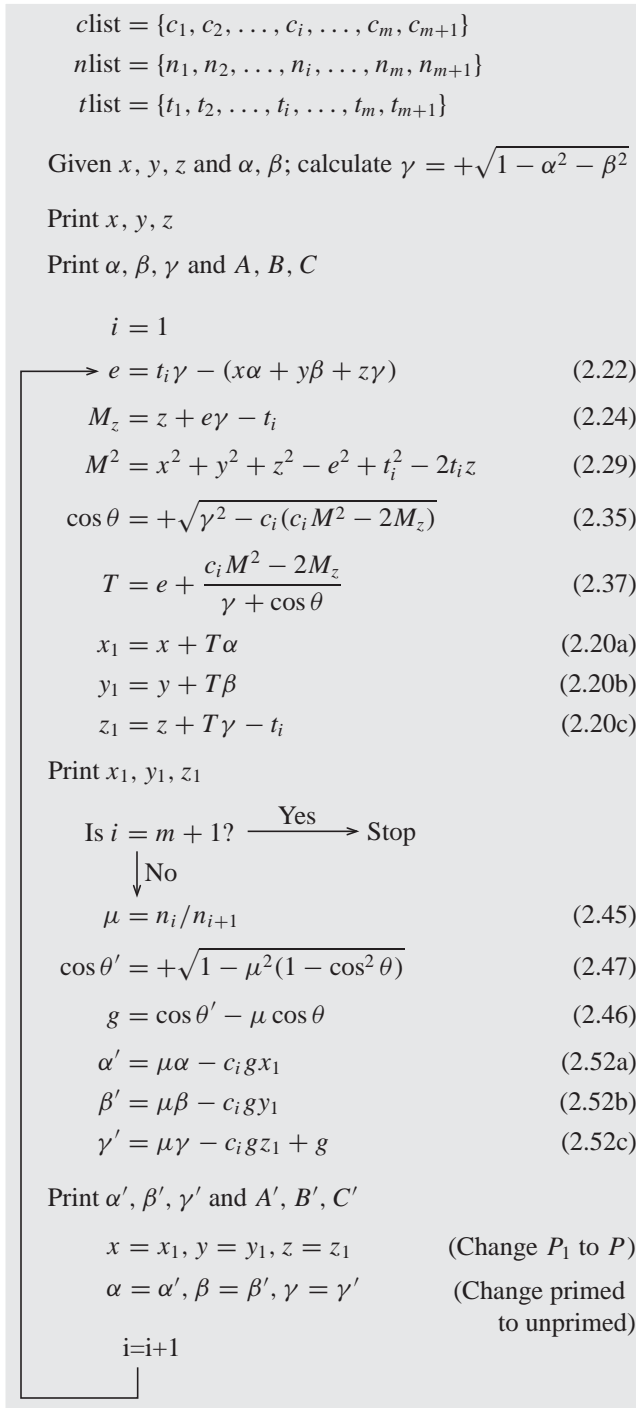


Figure 2.19 Basic flow chart for tracing skew rays.

outlines the way a computer program might be written in your favorite language to trace a ray through any number of refracting surfaces—the numbers in parentheses refer to the equation numbers where the equations were first derived in the preceding derivations. This flow chart also serves as a summary of all the important equations.

The generalized optical system that helps to describe the notation and the subscripts used in the flow chart is shown in Figure 2.20—it is drawn in two dimensions for simplicity. The notation is similar to that employed in Chapter 1, but has been simplified for use with a computer program. The last point is denoted by  $P'$ , and the last surface (here, imaginary) is plane because the last surface frequently is an image surface, which usually is a plane surface. Because of the  $-t_i$  in Equation 2.20c, the origin automatically moves to the vertex of the next refracting surface to keep the  $z$  coordinate the same order of magnitude as the  $x$  and  $y$  coordinates.

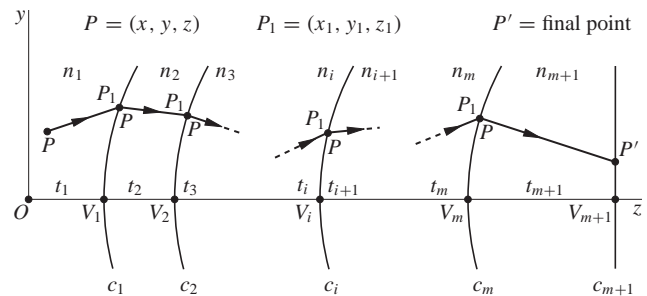


Figure 2.20 A generalized optical system to help understand the notation used in the flow chart for tracing skew rays.

#### Example 2.3.1 Exact ray tracing of a skew ray.

In Figure 2.21 we show a biconvex lens, and in Figure 2.22 we give the numerical values for this system. We now want

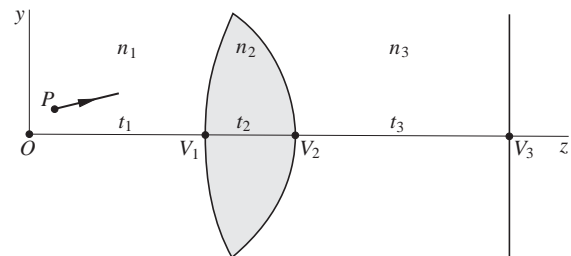


Figure 2.21

|                   | $r$ (mm) | $n$   | $t$ (mm) |
|-------------------|----------|-------|----------|
| $P : x = 2.00$ mm |          | 1.000 | 10.00    |
| $y = 1.00$        | 20.00    | 1.500 | 5.00     |
| $z = 2.00$        | -10.00   | 1.000 | 12.00    |
| $\alpha = 0.200$  |          |       |          |
| $\beta = 0.200$   | $\infty$ |       |          |

Figure 2.22

to implement the flow chart of Figure 2.19. By inspection of Figures 2.20, 2.21, and 2.22, we see that

$$\begin{aligned} \text{clist} &= \{0.05, -0.1, 0\} \\ \text{nlist} &= \{1, 1.5, 1\} \\ \text{tlist} &= \{10, 5, 12\} \end{aligned}$$

the initial values at point  $P$  are

$$\begin{aligned} x &= 2 \text{ mm} \\ y &= 1 \\ z &= 2 \end{aligned}$$

and the initial values of the two direction cosines are

$$\begin{aligned} \alpha &= 0.2 \\ \beta &= 0.2 \end{aligned}$$

We calculate  $\gamma$  as

$$\gamma = +\sqrt{1 - \alpha^2 - \beta^2} = 0.959166$$

Then we determine the initial direction angles to be

$$\begin{aligned} A &= 1.36944 \text{ rad} & B &= 1.36944 \text{ rad} & C &= 0.286757 \text{ rad} \\ &= 78.463 \text{ deg} & &= 78.463 \text{ deg} & &= 16.4299 \text{ deg} \end{aligned}$$

All our calculations are made with *Mathematica*'s 16 decimal digit precision and with its default display of six decimal digits, unless the digits to the right of the decimal point are trailing zeros, then they are not printed (such as the preceding values for  $A$  and  $B$  in deg).

Next, we set  $i = 1$  in the flow chart and calculate the quantities relating to translation from the initial point  $P$  to  $P_1$  on the first surface

$$\begin{aligned} e &= 7.07333 \text{ mm} \\ M_z &= -1.2155 \text{ mm} \\ M^2 &= 18.968 \text{ mm}^2 \\ \cos \theta &= 0.86662 \\ T &= 8.92426 \text{ mm} \end{aligned}$$

$$x_1 = 3.78485 \text{ mm} \quad y_1 = 2.78485 \text{ mm} \quad z_1 = 0.559848 \text{ mm}$$

and then refraction at the first surface

$$\begin{aligned} \mu &= 0.666667 \\ \cos \theta' &= 0.943052 \\ g &= 0.365305 \end{aligned}$$

$$\alpha' = 0.064202 \quad \beta' = 0.0824673 \quad \gamma' = 0.994524$$

From these values of  $\alpha'$ ,  $\beta'$ ,  $\gamma'$ , we obtain the direction angles

$$\begin{aligned} A' &= 1.50655 \text{ rad} & B' &= 1.48824 \text{ rad} & C' &= 0.104703 \text{ rad} \\ &= 86.319 \text{ deg} & &= 85.2696 \text{ deg} & &= 5.99905 \text{ deg} \end{aligned}$$

The diagram for this translation and refraction at the first surface is shown in Figure 2.23, where it is space on the diagram that determines how we round the values. The arc which passes through  $V_1$  and  $P_1$  is a circular arc on the spherical refracting surface—like a world line that passes through two cities on the earth.

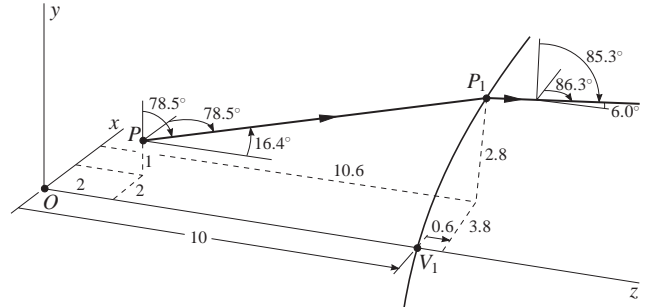


Figure 2.23

We now change the coordinates  $x_1, y_1, z_1$  of the point  $P_1$  to the  $x, y, z$  coordinates of point  $P$ , and the primed direction cosines to the unprimed values, as specified at the bottom of the flow chart, Figure 2.19. Then we increment  $i$  by one to get  $i = 2$  and repeat the calculations to obtain the values relating to translation to the second surface, and refraction at that surface. This time we simply give the pertinent results:

$$x_1 = 3.98453 \text{ mm} \quad y_1 = 3.04134 \text{ mm} \quad z_1 = -1.34704 \text{ mm}$$

$$\alpha' = -0.135022 \quad \beta' = -0.0528661 \quad \gamma' = 0.989431$$

$$\begin{aligned} A' &= 1.70623 \text{ rad} & B' &= 1.62369 \text{ rad} & C' &= 0.145515 \text{ rad} \\ &= 97.7599 \text{ deg} & &= 93.0304 \text{ deg} & &= 8.33742 \text{ deg} \end{aligned}$$

As before we draw the diagram to display these results in Figure 2.24; consistent with our earlier explanation, we note that the origin for these calculations is  $V_1$ .

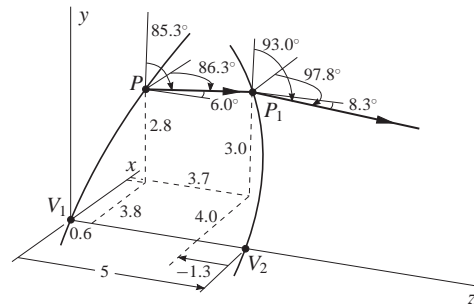


Figure 2.24

We are once again at the bottom of the flow chart: we change the subscripted values to unscripted ( $P_1$  to  $P$ ), and the primed to unprimed. We increment  $i$  by one to get  $i = 3$ ,

and following the arrow in the flow chart, we move to the calculation of  $e$  and the rest of the translation calculations to the final surface at  $V_3$ , which is the plane surface. We obtain

$$\begin{aligned} x_1 &= x' & y_1 &= y' & z_1 &= z' \\ &= 2.16314 \text{ mm} & &= 2.32819 \text{ mm} & &= 0 \text{ mm} \end{aligned}$$

Since  $i$  is now equal to  $m + 1$  (namely,  $i = m + 1 = 3$ ), the flow chart says to stop; we have performed the final calculations. As we did in Figure 2.20, we call this final point  $P'$  and change to primed coordinates  $(x', y', z')$ . The diagram that displays these final results is shown in Figure 2.25; we note that  $z'$  is zero, consistent with a point on a plane surface.

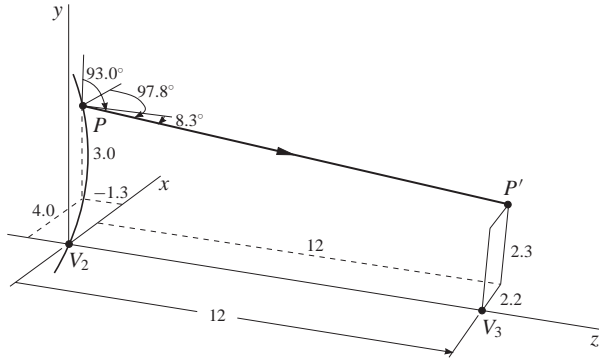


Figure 2.25

## 2.4 Spherical Aberration

### 2.4.1 Equations for description

We shall study spherical aberration by passing incident rays that are in the  $yz$  plane and parallel to the  $z$  axis (the symmetry axis) through the optical system. Rays that travel in the  $yz$  plane are in the meridional or tangential plane; such rays that travel close to the  $z$  axis are called paraxial rays, and were studied in Chapter 1. Paraxial rays that travel parallel to the symmetry axis as they enter an optical system emerge to pass through (or the backward extension passes through) an on-axis point called the paraxial focal point  $F'$ . However, the farther away from the symmetry axis these parallel rays are, the more they deviate from  $F'$ . This deviation is called spherical aberration, and we describe it with the help of Figure 2.26 in terms of quantities called longitudinal

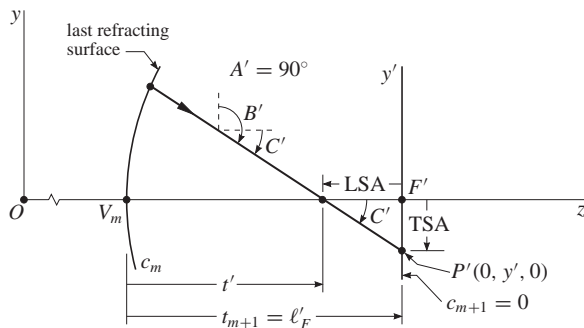


Figure 2.26

spherical aberration (LSA) and transverse spherical aberration (TSA); both these quantities are negative in the diagram. By inspection of Figure 2.26, we see that

$$\text{TSA} = y' \tag{2.54a}$$

$$\begin{aligned} \text{LSA} &= \frac{\text{TSA}}{\tan C'} = \text{TSA} \frac{\cos C'}{\sin C'} \\ &= \text{TSA} \frac{\cos C'}{\sqrt{1 - \cos^2 C'}} = \text{TSA} \frac{\gamma'}{\sqrt{1 - \gamma'^2}} \end{aligned} \tag{2.54b}$$

$$t' = \ell'_F + \text{LSA} \tag{2.54c}$$

where in the last equation we use a plus sign in front of LSA because it is negative when a ray crosses the  $z$  axis to the left of  $F'$ , as is the case in Figure 2.26. All the quantities needed in Equations 2.54 are easily calculated by using the equations in the flow chart of Figure 2.19, except for  $\ell'_F$ . To get  $\ell'_F$ , we use Equation 1.70 in Section 1.4—or we could trace a parallel ray very close to the symmetry axis, but it is good to review the earlier equations. To illustrate, we work some examples.

#### Example 2.4.1 Spherical aberration in a biconvex lens.

We analyze the lens of the earlier system in Example 2.3.1, except we now want to study the behavior of an incident ray parallel to the  $z$  axis and positioned a distance  $y$  from that axis, as shown in Figure 2.27. The ray begins at point  $P$  with the direction cosines  $\alpha, \beta$  equal to zero, as listed in Figure 2.28. As displayed in the diagram and in the  $t$  list, the point  $P$  is placed 10 mm to the left of vertex  $V_1$ ; actually, because the ray is parallel, how far to the left  $P$  is placed is arbitrary, 10 mm is just a convenient value. As indicated in the diagram, we trace

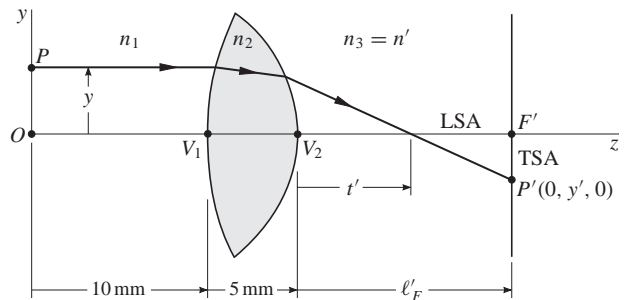


Figure 2.27

|                  | $r$ (mm) | $n$   | $t$ (mm)  |
|------------------|----------|-------|-----------|
| $P$ : $x = 0$ mm |          |       |           |
| $y = y$          | 20.00    | 1.000 | 10.00     |
| $z = 0$          | -10.00   | 1.500 | 5.00      |
| $\alpha = 0$     |          | 1.000 | $\ell'_F$ |
| $\beta = 0$      | $\infty$ |       |           |

Figure 2.28

the ray to a point  $P'$  on an imaginary plane a distance  $\ell'_F$  from  $V_2$ , where  $V_2$  marks the vertex of the last refracting surface of the system.

We perform this ray trace with the exact equations listed in the flow chart of Figure 2.19. Since we wish to calculate values of  $t'$ , LSA, TSA for selected values of  $y$ , we must insert Equations 2.54 at the “Stop” location in the flow chart. But first we must determine  $\ell'_F$ . The procedure we outlined in Example 1.5.2 in Chapter 1 provides a good guide for this calculation. We determine the system matrix

$$S_{21} = R_2 T_{21} R_1 = \begin{pmatrix} 0.833333 & -0.0708333 \\ 3.33333 & 0.916667 \end{pmatrix}$$

and read off the two Gaussian constants we need

$$a = 0.0708333 \\ c = 0.916667$$

Then

$$\ell'_F = n' \frac{c}{a} = (1) \frac{0.916667}{0.0708333} = 12.9412 \text{ mm}$$

and we construct the first line of our table in Figure 2.29: the values of  $t'$ , LSA, TSA for  $y = 0$ . Now that we have a value for  $\ell'_F$ , we can fill out the  $t$ list, and obtain a complete listing of the data for our system:

$$clist = \{0.05, -0.1, 0\} \\ nlist = \{1, 1.5, 1\} \\ tlist = \{10, 5, 12.9412\}$$

For the values  $y = 0.5, 1, 1.5, \dots, 5$  mm, we determine the corresponding values of  $t'$ , LSA, TSA by running our modified flow chart (see the beginning of this paragraph) with *Mathematica* (or you use your own program that you have written). As usual, the values in the table are displayed with six decimal digits, unless the digits to the right of the decimal point are trailing zeros, then they are not printed.

| $y$ (mm) | $t'$ (mm) | LSA (mm)   | TSA (mm)    |
|----------|-----------|------------|-------------|
| 0.       | 12.9412   | 0.         | 0.          |
| 0.5      | 12.9044   | -0.0367786 | -0.00130559 |
| 1.       | 12.7932   | -0.147978  | -0.0105802  |
| 1.5      | 12.6049   | -0.336274  | -0.0365     |
| 2.       | 12.3348   | -0.606423  | -0.0893093  |
| 2.5      | 11.9754   | -0.965788  | -0.182053   |
| 3.       | 11.5159   | -1.42527   | -0.332577   |
| 3.5      | 10.9402   | -2.001     | -0.567149   |
| 4.       | 10.2237   | -2.71749   | -0.927747   |
| 4.5      | 9.32676   | -3.61442   | -1.48891    |
| 5.       | 8.17735   | -4.76383   | -2.40512    |

Figure 2.29

**Example 2.4.2 The planoconvex lens.**

In this example, we shall study spherical aberration for a planoconvex lens: first, with the convex surface facing the incident rays parallel to the symmetry axis; second, with the plane surface facing the parallel rays.

1) **Convex surface faces incident rays.** The diagram in Figure 2.30 shows a planoconvex lens with the convex surface facing a parallel ray a distance  $y$  above the  $z$  axis. The numerical properties of the lens are listed in the table of Figure 2.31.

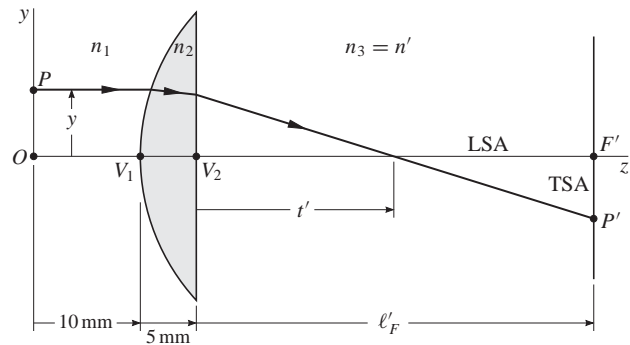


Figure 2.30

|                        | $r$ (mm) | $n$   | $t$ (mm)  |
|------------------------|----------|-------|-----------|
| $P : x = 0 \text{ mm}$ |          | 1.000 | 10.00     |
| $y = y$                | 20.00    | 1.500 | 5.00      |
| $z = 0$                | $\infty$ | 1.000 | $\ell'_F$ |
| $\alpha = 0$           |          |       |           |
| $\beta = 0$            | $\infty$ |       |           |

Figure 2.31

We follow the procedure of the previous example: find the system matrix

$$S_{21} = R_2 T_{21} R_1 = \begin{pmatrix} 1. & -0.025 \\ 3.33333 & 0.916667 \end{pmatrix}$$

read off the two Gaussian constants we need

$$a = 0.025 \\ c = 0.916667$$

and calculate

$$\ell'_F = n' \frac{c}{a} = (1) \frac{0.916667}{0.025} = 36.6667 \text{ mm} \\ f' = \frac{n'}{a} = \frac{1}{0.025} = 40 \text{ mm}$$

where knowledge of the focal length  $f'$  will be helpful in this example of comparing properties of the two orientations of the same lens.



Now that we know the value of  $\ell'_F$ , we can construct the data lists

$$\begin{aligned} clist &= \{0.05, 0, 0\} \\ nlist &= \{1, 1.5, 1\} \\ tlist &= \{10, 5, 36.6667\} \end{aligned}$$

and fill in the values which correspond to  $y = 0$  mm in the first line of the spherical aberration table of Figure 2.32. The values of  $t'$ , LSA, TSA corresponding to  $y = 1, 2, \dots, 10$  mm are calculated with the flow chart in Figure 2.19 and Equations 2.54, and are displayed in Figure 2.32.

| y (mm) | $t'$ (mm) | LSA (mm)   | TSA (mm)     |
|--------|-----------|------------|--------------|
| 0.     | 36.6667   | 0.         | 0.           |
| 1.     | 36.6381   | -0.0286079 | -0.000716018 |
| 2.     | 36.552    | -0.114672  | -0.00576005  |
| 3.     | 36.4077   | -0.258923  | -0.0196227   |
| 4.     | 36.204    | -0.462618  | -0.0471348   |
| 5.     | 35.9391   | -0.727598  | -0.0936764   |
| 6.     | 35.6103   | -1.05638   | -0.165442    |
| 7.     | 35.2144   | -1.45229   | -0.269794    |
| 8.     | 34.747    | -1.91969   | -0.415756    |
| 9.     | 34.2024   | -2.46423   | -0.614736    |
| 10.    | 33.5734   | -3.09331   | -0.88162     |

Figure 2.32 Convex surface faces the incident rays.

**2) Plane surface faces incident rays.** We rotate the lens in Figure 2.30 so that the plane surface faces the incident rays that are parallel to the symmetry axis. We show this new lens orientation in Figure 2.33 with the corresponding numerical properties listed in Figure 2.34.

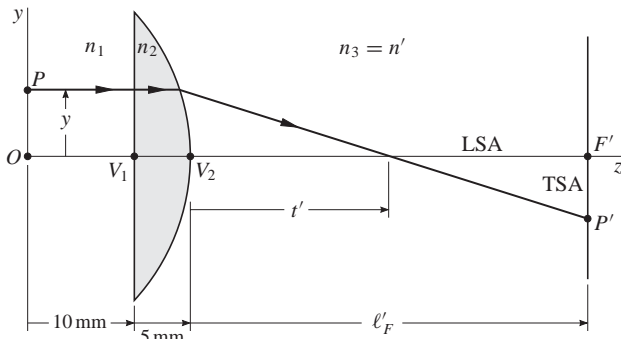


Figure 2.33

| $r$ (mm) | $n$   | $t$ (mm)  |
|----------|-------|-----------|
| $\infty$ | 1.000 | 10.00     |
| -20.00   | 1.500 | 5.00      |
| $\infty$ | 1.000 | $\ell'_F$ |

$P : x = 0$  mm  
 $y = y$   
 $z = 0$   
 $\alpha = 0$   
 $\beta = 0$

Figure 2.34

In the usual way, we calculate the system matrix  $S$ : we find  $a = 0.025$  and  $c = 1$  so that  $\ell'_F = n'c/a = 40$  mm and  $f' = n'/a = 40$  mm. Although the  $\ell'_F$  is different for this orientation, the focal length  $f'$  is the same as before. The data lists are

$$\begin{aligned} clist &= \{0, -0.05, 0\} \\ nlist &= \{1, 1.5, 1\} \\ tlist &= \{10, 5, 40\} \end{aligned}$$

and we calculate the spherical aberration values listed in the table of Figure 2.35.

| y (mm) | $t'$ (mm) | LSA (mm)  | TSA (mm)    |
|--------|-----------|-----------|-------------|
| 0.     | 40.       | 0.        | 0.          |
| 1.     | 39.8874   | -0.112623 | -0.00282176 |
| 2.     | 39.548    | -0.451988 | -0.0227999  |
| 3.     | 38.9773   | -1.02269  | -0.0782602  |
| 4.     | 38.1672   | -1.83281  | -0.19007    |
| 5.     | 37.1054   | -2.89455  | -0.383481   |
| 6.     | 35.7745   | -4.2255   | -0.690899   |
| 7.     | 34.1494   | -5.85056  | -1.15642    |
| 8.     | 32.1945   | -7.80545  | -1.84394    |
| 9.     | 29.8567   | -10.1433  | -2.85317    |
| 10.    | 27.0514   | -12.9486  | -4.35526    |

Figure 2.35 Plane surface faces the incident rays.

**Comparison of the two orientations.** We now compare the spherical aberration for the two orientations of the planoconvex lens. We plot the TSA values in Figures 2.32 and 2.35 versus  $y$ , and draw smooth curves through the points, as displayed in Figure 2.36. Curve 1 shows the TSA behavior for the convex side facing the incident rays, curve 2 shows the similar behavior for the plane side facing the rays. Clearly, the spherical aberration is smaller for curve 1. Therefore, just a simple change in the orientation of the lens can reduce spherical aberration.

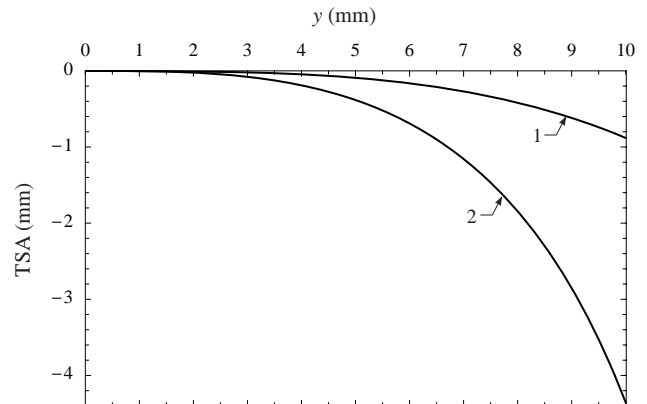
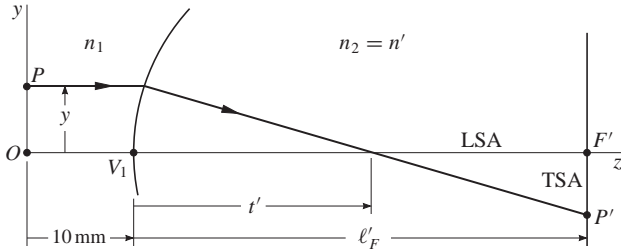


Figure 2.36

**Example 2.4.3 A single surface.**

As a last example, we study the spherical aberration of a single convex surface. The results of this example will be useful in a later chapter. We diagram this optical system in Figure 2.37, and give the numerical information for the system in Figure 2.38.



**Figure 2.37**

|                        |                  |       |                  |
|------------------------|------------------|-------|------------------|
| $P : x = 0 \text{ mm}$ | $r \text{ (mm)}$ | $n$   | $t \text{ (mm)}$ |
| $y = y$                | 20.00            | 1.000 | 10.00            |
| $z = 0$                | $\infty$         | 1.500 | $l'_F$           |
| $\alpha = 0$           |                  |       |                  |
| $\beta = 0$            |                  |       |                  |

**Figure 2.38**

We determine the system matrix

$$S_1 = R_1 = \begin{pmatrix} 1 & -0.025 \\ 0 & 1 \end{pmatrix}$$

read off the two Gaussian constants we need

$$a = 0.025 \quad c = 1$$

calculate

$$l'_F = n' \frac{c}{a} = (1.5) \frac{1}{0.025} = 60 \text{ mm}$$

and construct the first line of the table in Figure 2.39. The data for this system is

$$clist = \{0.05, 0\} \quad nlist = \{1, 1.5\} \quad tlist = \{10, 60\}$$

and we then use the flow chart in Figure 2.19 and Equations 2.54 to calculate the values associated with spherical aberration for  $y = 1, 2, \dots, 5$ , as listed below:

| $y \text{ (mm)}$ | $t' \text{ (mm)}$ | LSA (mm)   | TSA (mm)     |
|------------------|-------------------|------------|--------------|
| 0.               | 60.               | 0.         | 0.           |
| 1.               | 59.9667           | -0.0333496 | -0.000556367 |
| 2.               | 59.8664           | -0.133594  | -0.00447055  |
| 3.               | 59.6987           | -0.301326  | -0.0151999   |
| 4.               | 59.4624           | -0.537556  | -0.0364084   |
| 5.               | 59.1563           | -0.843747  | -0.0720891   |

**Figure 2.39** Single convex surface.

**2.4.2 Shaping (or bending) a lens**

Reducing spherical aberration through orientation, as described in Example 2.4.2, is a particular case of a more general technique called shaping or bending the lens. In this method, the lens is shaped by changing the radii while holding other properties of the lens constant, or approximately constant. To keep track of the lens shape, we define a shape factor  $S$  as

$$S = \frac{r_2 + r_1}{r_2 - r_1} = \frac{c_1 + c_2}{c_1 - c_2} \tag{2.55}$$

Although we have already used  $S$  to denote a system matrix, the context tells us which quantity the symbol represents.

To obtain an awareness of what shapes correspond to particular values of  $S$  for a converging lens, we draw the lens diagrams in Figure 2.40, and also give some information about the radii below each lens shape. We see that  $S = 0$  represents an equiconvex lens; nonzero values of  $S$  describe the deviation of the lens from symmetry.

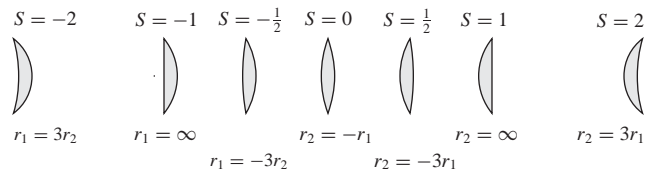


**Figure 2.40**

As we shape the lens, it is easy to keep the index of refraction and the thickness of the lens constant. It is not as easy to hold the height and focal length  $f'$  constant. However, in the region of usual interest, we find that the lens height does not vary much, and that it is sufficient (and much simpler) to hold the thin-lens  $f'$  constant, as given by Equation 1.158.

We begin our equation development by writing the thin-lens  $f'$  of Equation 1.158 in terms of the curvatures  $c$  and the index of refraction  $n_2$  of the lens (remember  $n'_1 = n_2$ ):

$$\frac{1}{f'} = (n_2 - 1)(c_1 - c_2) \tag{2.56}$$

We take the system of equations composed of Equation 2.56 and the  $c$  form of Equation 2.55, and then solve this system for  $c_1$  and  $c_2$ :

$$c_1 = \frac{S + 1}{2(n_2 - 1)f'} \tag{2.57a}$$

$$c_2 = \frac{S - 1}{2(n_2 - 1)f'} \tag{2.57b}$$

We now observe that our last two equations permit us to calculate  $c_1$  and  $c_2$  when we are given  $n_2$ ,  $f'$ , and  $S$ , which is the situation we desire.

We show how to implement these equations for calculating TSA versus  $S$  in the flow chart outline in Figure 2.41. This flow chart describes how to determine the TSA for different values of  $S$  with an incident ray that is parallel to and a given height  $y_0$  from the  $z$  axis. We call the flow chart an outline because we have omitted a number of pertinent steps for obtaining our goal: a graph of TSA versus  $S$  as well as the procedure needed to determine the  $S$  value for which TSA gives the smallest spherical aberration. This work is left as a problem for the reader, since the routine written may depend on the computer software used.

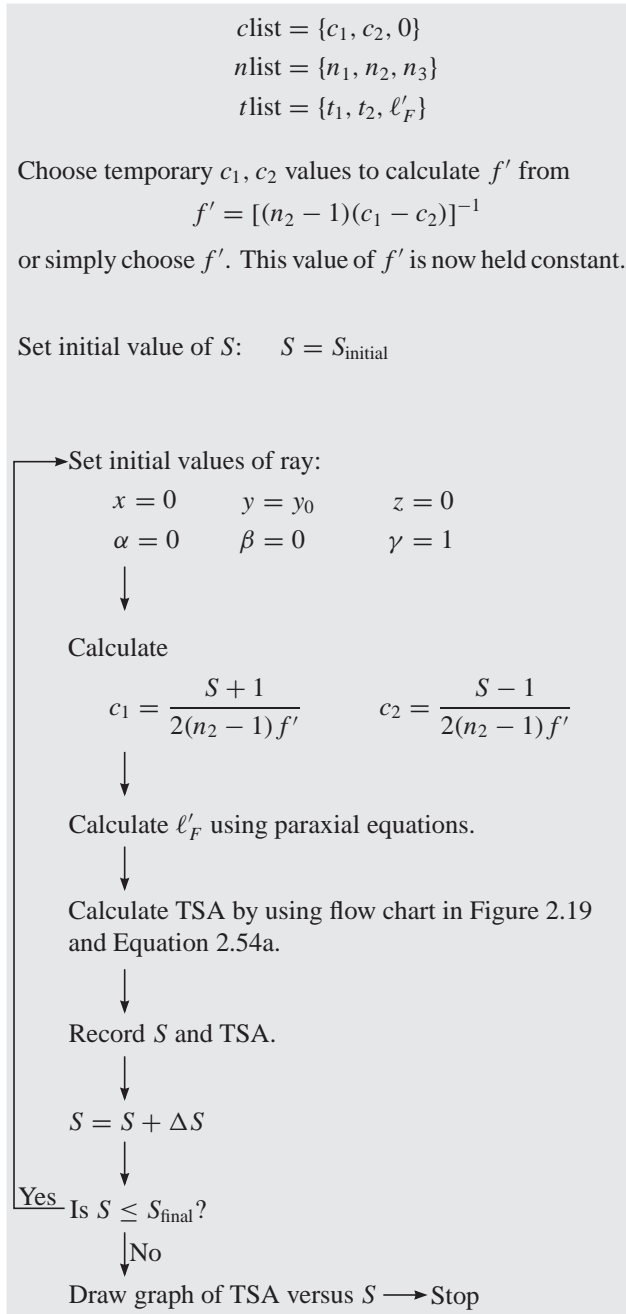


**Figure 2.41** Flow chart outline for TSA versus  $S$ .

**Example 2.4.4 Investigation of TSA versus  $S$ .**

We apply shaping to the lens of Example 2.4.2, Figure 2.30. Keeping in mind the flow chart of Figure 2.41, we use the data for this lens in Figure 2.31 to construct

$$clist = \{c_1, c_2, 0\}$$

$$nlist = \{1, 1.5, 1\}$$

$$tlist = \{10, 5, \ell'_F\}$$

We do not give values for  $c_1, c_2$  in the  $clist$  because these quantities will be recalculated for every new value of  $S$ . But we must give them temporary values to get the  $f'$  that is held constant. From the data for this lens in Figure 2.31, we see that  $c_1 = 1/r_1 = 0.05$ ,  $c_2 = 0$ , and  $n_2 = 1.5$ ; thus  $f' = 40$  mm by Equation 2.56. For the other quantities that need values, we set  $y_0 = 10$  mm,  $S_{initial} = -1.5$ ,  $S_{final} = 2$ , and  $\Delta S = 0.01$ .

Implementing the flow chart with a computer program, we obtain the graph of TSA versus  $S$  shown in Figure 2.42. To determine the lens properties when spherical aberration is smallest, we see by inspection of the graph that this value occurs at the  $S$  where TSA is a maximum (or when  $|TSA|$  is a minimum). Inserting steps into the flow chart to determine this information, we find that the maximum occurs at

$$S = 0.62 \quad \text{for which} \quad TSA = -0.750797 \text{ mm}$$

and

$$c_1 = 0.0405 \text{ mm}^{-1}, \quad c_2 = -0.0095 \text{ mm}^{-1}$$

or

$$r_1 = 24.6914 \text{ mm}, \quad r_2 = -105.263 \text{ mm}$$

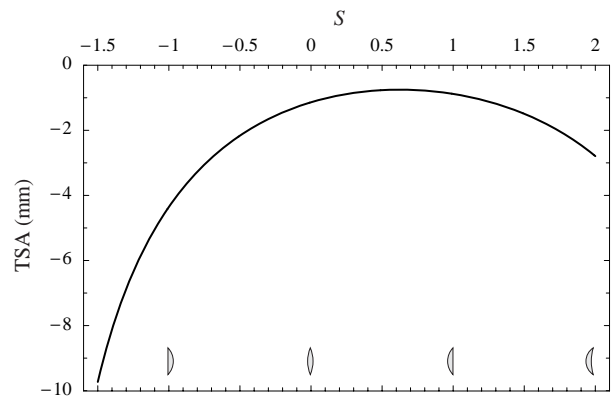


**Figure 2.42**

Observe that in working this example, we implemented the “Record  $S$  and TSA” of the flow chart in Figure 2.41 for all the calculated points, which produced a rather large number of  $(S, TSA)$  value pairs. If this large number causes a problem, it is possible to change the program to work with fewer pairs.

As a final investigation, we take the lens of the previous example that produced the smallest spherical aberration, and exactly trace a ray through the lens paying special attention to the deviation of the ray as it refracts at each surface. The data lists are

$$\begin{aligned} clist &= \{0.0405, -0.0095, 0\} \\ nlist &= \{1, 1.5, 1\} \\ tlist &= \{10, 5, \ell'_F\} \end{aligned}$$

and the ray we trace is the usual one: an incident ray parallel to the  $z$  axis at a distance 10 mm above it. With the customary paraxial techniques, we find that  $\ell'_F = 37.7846$  mm. To determine the deviation angles (the angle between the ray direction after refraction and the ray direction before refraction), we must insert some statements into the flow chart of Figure 2.19. Fortunately, this effort is not difficult, and we obtain the results shown in the diagram of Figure 2.43. We make the interesting observation that the two deviation angles are approximately the same.

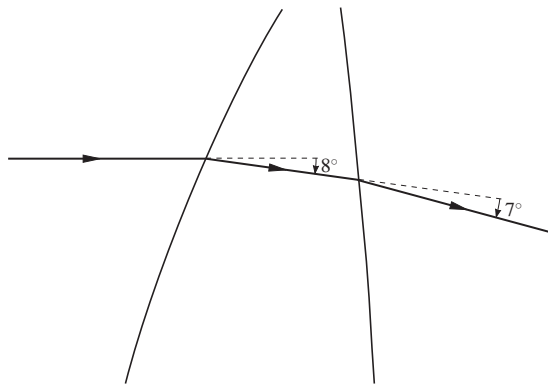


Figure 2.43

This result is quite important because it is found that in general, even when there are more refracting surfaces, spherical aberration is smallest when all the deviation angles are approximately equal. Now we can understand why the planar-convex lens of Example 2.4.2 produced the smaller spherical aberration when the convex surface faced the incident rays: nonzero ray deviation occurred at each of the two surfaces. When the planar surface faced the incident rays, ray deviation only occurred at the second surface.

### 2.4.3 The radius of a converging lens

It is frequently important to know the radius  $R$  (height above the symmetry axis) or diameter  $D$  of a converging lens. Unfortunately, the ray tracing formulas do not always indicate when a ray misses a lens in an optical system; for example, when it travels above the converging lens in the doublet we are going to analyze in the next section. For convenience, we shall imagine a converging lens to have a sharp edge at the circumference; in fact, we have drawn our diagrams in

this text under this assumption. In actual practice, however, a converging lens is made so its edge or rim thickness is about 1 mm or more for safety and to make chipping less likely. Thus, the clear radius of a lens is a little less than the  $R$  we are calculating. Furthermore, the lens is usually held in a holder, which makes the clear radius yet smaller. We are ignoring these practical matters for simplicity.

The converging lens of thickness  $t$  that we consider for the derivation of its radius  $R$  is shown in Figure 2.44, where we show the top half of the lens. The diameter  $D$  of this lens is then  $2R$ . We have drawn this diagram such that all the

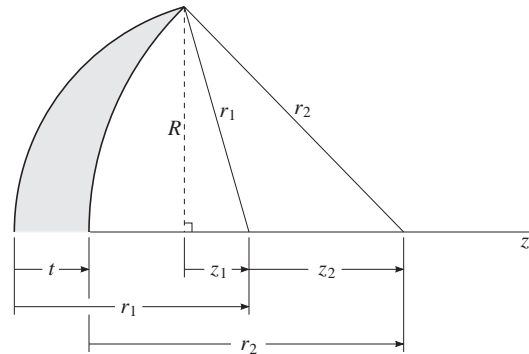


Figure 2.44

quantities shown are positive to make the derivation easier. By inspection, we see that

$$r_1 + z_2 = t + r_2$$

or

$$z_2 = r_2 - r_1 + t \tag{2.58}$$

By using Pythagorean's theorem on the two right triangles in the diagram of Figure 2.44, we obtain

$$R^2 + z_1^2 = r_1^2 \tag{2.59a}$$

$$R^2 + (z_1 + z_2)^2 = r_2^2 \tag{2.59b}$$

One way to write the solution to this system of equations is

$$R = \sqrt{r_1^2 - z_1^2} \tag{2.60a}$$

where

$$z_1 = \frac{r_2^2 - r_1^2 - z_2^2}{2z_2} \tag{2.60b}$$

and

$$z_2 = r_2 - r_1 + t \tag{2.60c}$$

We rewrote Equation 2.58 as Equation 2.60c for convenience.

Another way to write the solution is as a single equation by substituting Equations 2.60b and 2.60c into Equation 2.60a: after simplification, we get

$$R = \frac{1}{2} \sqrt{\frac{t(2r_1 - t)(2r_2 + t)(2r_2 - 2r_1 + t)}{(r_2 - r_1 + t)^2}} \tag{2.61}$$

It is best to leave  $(r_2 - r_1 + t)^2$  inside the square root to avoid possible minus sign problems.

The previous Equation 2.61 is especially useful for determining the formulas for a planoconvex lens. First, when  $r_2 \rightarrow \infty$ , we obtain

$$R = \sqrt{t(2r_1 - t)} \quad (2.62)$$

Second, when  $r_1 \rightarrow \infty$ , we have

$$R = \sqrt{t(-2r_2 - t)} \quad (2.63)$$

---

**Example 2.4.5 Radius of a biconvex lens.**

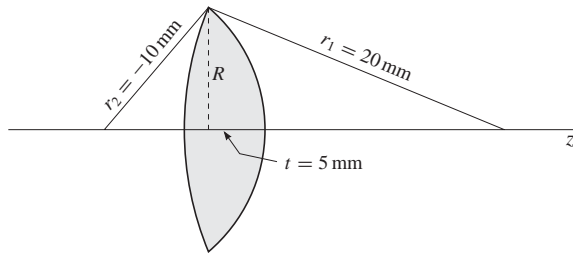


**Figure 2.45**

As our first example, we take the lens from Example 2.4.1, and redraw it in Figure 2.45. Substituting the data from the diagram into Equations 2.60, we calculate

$$z_2 = -25 \text{ mm} \quad z_1 = 18.5 \text{ mm}$$

$$R = \sqrt{r_1^2 - z_1^2} = \sqrt{(20)^2 - (18.5)^2} = 7.60 \text{ mm}$$

---

**Example 2.4.6 Radius of a planoconvex lens.**

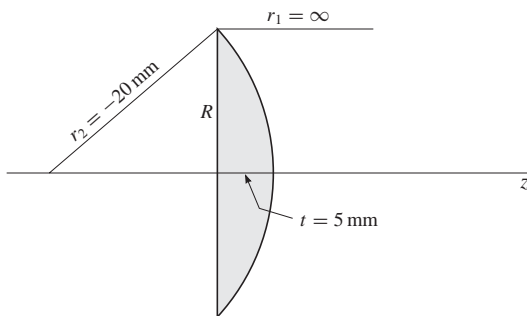


**Figure 2.46**

For the planoconvex lens in Figure 2.46, which is the lens used in Figure 2.33 of Example 2.4.2, we have

$$R = \sqrt{t(-2r_2 - t)} = \sqrt{5(-2(-20) - 5)} = 13.23 \text{ mm}$$


---

**Example 2.4.7 Radius of a shaped biconvex lens.**

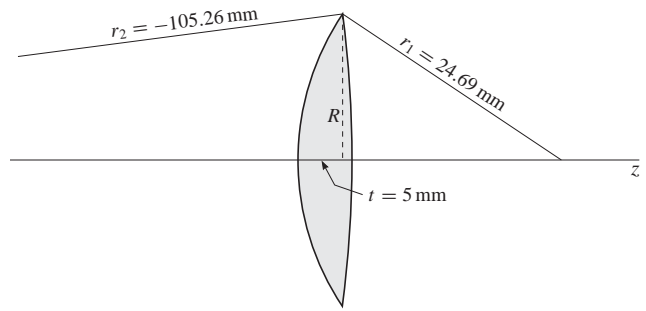


**Figure 2.47**

In Example 2.4.4, we shaped a lens of thickness 5 mm to give a value of TSA close to zero: we found that  $r_1 = 24.69 \text{ mm}$  and  $r_2 = -105.26 \text{ mm}$  (rounding the values to two decimal places). We draw this lens in Figure 2.47, and calculate the radius  $R$  with the help of Equations 2.60:

$$z_2 = -124.95 \text{ mm} \quad z_1 = 20.58 \text{ mm}$$

$$R = \sqrt{r_1^2 - z_1^2} = \sqrt{(24.69)^2 - (20.58)^2} = 13.64 \text{ mm}$$

---

**Example 2.4.8 Radius of the biconvex lens used in the next section.**

In the next section, we shall consider another way of reducing spherical aberration: with a doublet. One of the lenses in the doublet is a converging lens, a biconvex lens. This lens has a thickness of 5 mm with radii of  $r_1 = 27.11 \text{ mm}$  and  $r_2 = -15.25 \text{ mm}$ . Since we are calculating radii  $R$  in the current examples, it is convenient to consider this lens here.

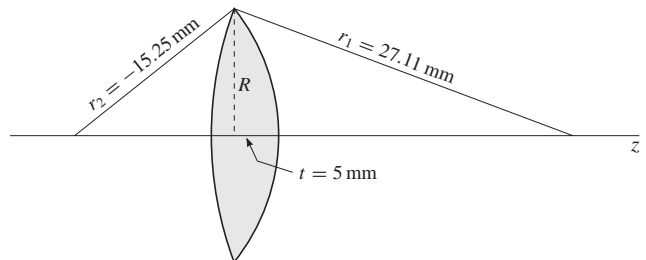


**Figure 2.48**

Substituting the values of  $r_1 = 27.11 \text{ mm}$ ,  $r_2 = -15.25 \text{ mm}$ , and  $t = 5 \text{ mm}$  into Equations 2.60, we get

$$z_2 = -37.36 \text{ mm} \quad z_1 = 25.40 \text{ mm}$$

$$R = \sqrt{r_1^2 - z_1^2} = \sqrt{(27.11)^2 - (25.40)^2} = 9.47 \text{ mm}$$


---

### 2.4.4 Spherical aberration of a doublet

1) **Lens with minimum |TSA|.** As a prelude to our investigation of the spherical aberration of a doublet, we shall first look at the spherical aberration of the lens examined in Example 2.4.4. In that example, we found the lens shape  $S$  for a biconvex lens which yielded a maximum value for its TSA (or a minimum value for its |TSA|). We want to analyze the spherical aberration for this shaped lens following the procedure of Example 2.4.1, and then do one additional thing: draw a graph of TSA versus  $y$  as in Figure 2.36.

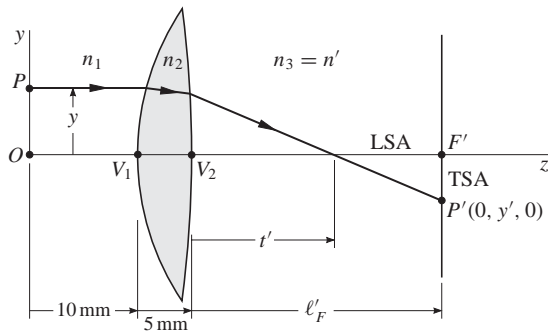


Figure 2.49

| $P : x = 0 \text{ mm}$ | $c \text{ (mm}^{-1}\text{)}$ | $n$   | $t \text{ (mm)}$ |
|------------------------|------------------------------|-------|------------------|
| $y = y$                | 0.0405                       | 1.000 | 10.00            |
| $z = 0$                | -0.0095                      | 1.500 | 5.00             |
| $\alpha = 0$           |                              | 1.000 | $l'_F$           |
| $\beta = 0$            | 0                            |       |                  |

Figure 2.50

We begin our analysis of spherical aberration by drawing the diagram in Figure 2.49, and list the properties of the system in Figure 2.50. We note that in the table we list the curvature  $c$  values in the first column of the table rather than the  $r$  values for the simple reason that the  $c$  values are simpler (see the  $c$  and  $r$  values above Figure 2.42). With the usual paraxial methods (see Example 2.4.1), we calculate  $l'_F = 37.7846 \text{ mm}$ . We now make the listing of data for this system as

$$\begin{aligned}
 c\text{list} &= \{0.0405, -0.0095, 0\} \\
 n\text{list} &= \{1, 1.5, 1\} \\
 t\text{list} &= \{10, 5, 37.7846\}
 \end{aligned}$$

Following the method in Example 2.4.1, we use the flow chart in Figure 2.19 to exactly trace rays of the type shown in Figure 2.49 to the point  $P'$  on the focal plane. Then the Equations 2.54 are used to calculate the values of  $t'$ , LSA, TSA, and listed in the table of Figure 2.51—except for the first row  $y = 0$  of the table, where  $t' = l'_F = 37.7846 \text{ mm}$ , and both LSA and TSA are zero.

| $y \text{ (mm)}$ | $t' \text{ (mm)}$ | LSA (mm)   | TSA (mm)     |
|------------------|-------------------|------------|--------------|
| 0.               | 37.7846           | 0.         | 0.           |
| 1.               | 37.759            | -0.0256367 | -0.000633251 |
| 2.               | 37.6818           | -0.102755  | -0.00508973  |
| 3.               | 37.5526           | -0.231989  | -0.0173131   |
| 4.               | 37.3702           | -0.414422  | -0.041497    |
| 5.               | 37.133            | -0.651632  | -0.0822333   |
| 6.               | 36.8388           | -0.945754  | -0.144693    |

Figure 2.51

Finally, we plot the  $(y, \text{TSA})$  values from the table, and then draw a smooth curve through the points to obtain the TSA versus  $y$  graph in Figure 2.52.

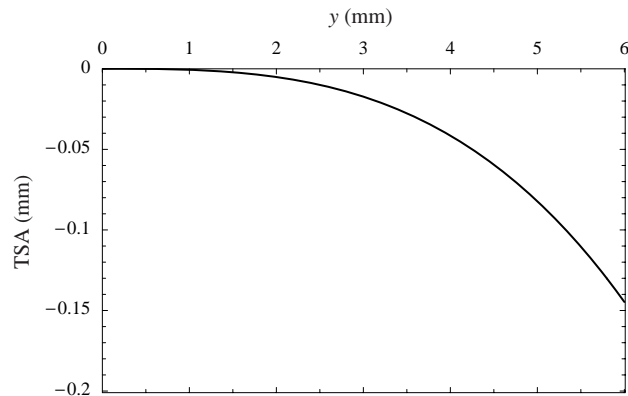


Figure 2.52 The shaped lens.

2) **A doublet.** Carefully chosen doublets have a much smaller spherical aberration than even a well-shaped single lens. The doublet we shall investigate is composed of a converging and diverging lens: It is drawn in Figure 2.53 and its corresponding data is shown in Figure 2.54.

The indices of refraction of the two lenses in the doublet are different; namely,  $n_2 = 1.5$  and  $n_3 = 1.6$ . These two indices are different to provide one of the requirements to cause the doublet to have the small spherical aberration we desire. We choose the paraxial focal length  $f' = 40 \text{ mm}$ , in agreement with the  $f'$  chosen for the shaped lens of Figure 2.49 and Example 2.4.4. Next, we search for appropriate values of  $r_1, r_2, r_3$ . The ones that work quite well for our doublet are shown in the  $r$  column of Figure 2.54—the procedure for finding these  $r$  values is beyond the scope of this text. The thickness of the lenses does not have a strong influence on the spherical aberration properties of the doublet; we simply choose 5 mm as a convenient thickness for both lenses.

Again, our job is to determine the Gaussian constants for the doublet optical system from which we calculate  $l'_F$ . Then we trace a ray through the doublet with the ray starting out parallel to the symmetry axis, and calculate the  $t'$ , LSA, TSA at the  $F'$  focal plane. We repeat this procedure for several rays for different  $y$  values (see Figure 2.53). Finally, we draw a TSA versus  $y$  graph similar to that in Figure 2.52.

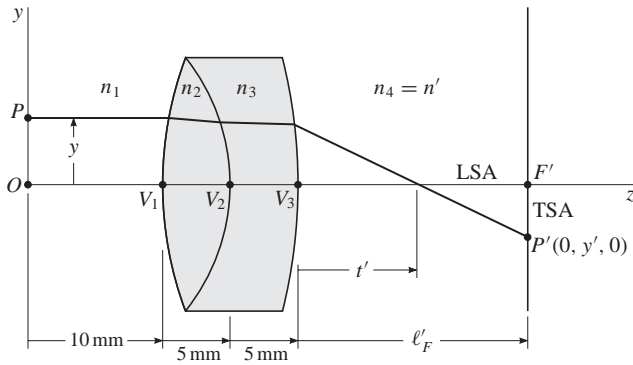


Figure 2.53

| $r$ (mm) | $n$   | $t$ (mm) |
|----------|-------|----------|
| 27.11    | 1.000 | 10.00    |
| -15.25   | 1.500 | 5.00     |
| -45.75   | 1.600 | 5.00     |
| $\infty$ | 1.000 | $l'_F$   |

$P : x = 0 \text{ mm}$   
 $y = y$   
 $z = 0$   
 $\alpha = 0$   
 $\beta = 0$

Figure 2.54

With the usual paraxial methods, we calculate for the doublet,  $l'_F = 37.3587 \text{ mm}$ , and then construct the data lists for the doublet (the *clist* values are the reciprocals of the *r* values in Figure 2.54):

$$\begin{aligned} \text{clist} &= \{0.0368868, -0.0655738, -0.0218579, 0\} \\ \text{nlist} &= \{1, 1.5, 1.6, 1\} \\ \text{tlist} &= \{10, 5, 5, 37.3587\} \end{aligned}$$

Running the flow chart of Figure 2.19, which has been modified at the end to calculate the  $t'$ , LSA, TSA (as we have

described previously), we get the table in Figure 2.55. The graph of TSA versus  $y$  is shown in Figure 2.56.

| $y$ (mm) | $t'$ (mm) | LSA (mm)    | TSA (mm)     |
|----------|-----------|-------------|--------------|
| 0.       | 37.3587   | 0.          | 0.           |
| 1.       | 37.3542   | -0.00447098 | -0.000107763 |
| 2.       | 37.3421   | -0.0165481  | -0.000798549 |
| 3.       | 37.5526   | -0.0319605  | -0.0023173   |
| 4.       | 37.316    | -0.04262    | -0.00412897  |
| 5.       | 37.3239   | -0.0347926  | -0.00422309  |
| 6.       | 37.3731   | 0.0144488   | 0.00210885   |

Figure 2.55

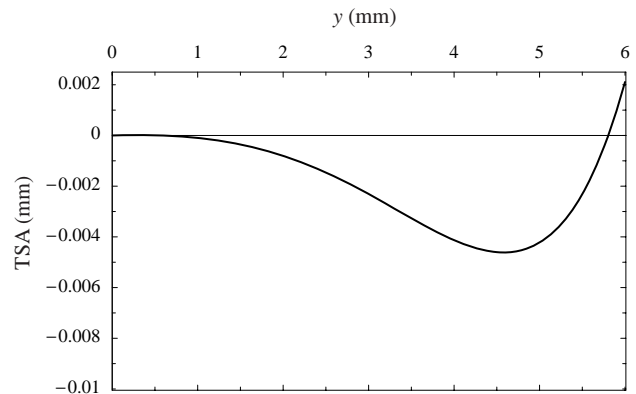


Figure 2.56 The doublet.

**3) Summary.** Comparing the two graphs (Figures 2.52 and 2.56), we see that the nature of the TSA curve for the doublet is entirely different from that of the shaped lens. Even more important, the TSA values for the doublet are roughly more than a factor of 10 smaller than those for the shaped lens. The reason this behavior takes place is that a diverging lens tends to have properties that are opposite to those of a converging one.

## PROBLEMS

- 2.1 Suppose  $A = 120 \text{ deg}$ ,  $B = 50 \text{ deg}$ ,  $C = 54.5237 \text{ deg}$ . (a) Find the corresponding direction cosines. (b) Show that the direction cosines obey Equation 2.4.
- 2.2 Suppose  $A = 1.5 \text{ rad}$ ,  $B = 0.68 \text{ rad}$ ,  $C = 0.89592 \text{ rad}$ . (a) Find the corresponding direction cosines. (b) Show that the direction cosines obey Equation 2.4.
- 2.3 Suppose that two of the direction cosines are given as  $\alpha = 0.5$ ,  $\beta = 0.5$  for a forward directed ray. (a) Calculate  $\gamma$  from Equation 2.4. (b) Find the corresponding direction angles. (c) Draw a rough graph of a vector that has these direction angles.
- 2.4 A vector has the two direction angles  $A = 60 \text{ deg}$  and  $B = 45 \text{ deg}$ . (a) Determine the direction angle  $C$ . (b) Draw a rough graph of this vector showing its direction angles.
- 2.5 (a) What are the direction angles of a vector parallel to the  $x$  axis, and (b) the direction cosines?
- 2.6 Suppose a vector is given in rectangular form by the expression  $\mathbf{a} = 2\mathbf{i} - \mathbf{j} - 3\mathbf{k}$ . (a) Calculate the magnitude of this vector. (b) Find the unit vector  $\mathbf{u}$  having the same direction as  $\mathbf{a}$ . (c) State the direction cosines of  $\mathbf{u}$ . (d) Determine the direction angles of  $\mathbf{u}$ .

2.7 If  $\mathbf{a} = 3\mathbf{i} - \mathbf{j} - 4\mathbf{k}$ ,  $\mathbf{b} = -2\mathbf{i} + 4\mathbf{j} - 3\mathbf{k}$ ,  $\mathbf{c} = \mathbf{i} + 2\mathbf{j} - \mathbf{k}$ , (a) find the magnitude of  $\mathbf{a} + \mathbf{b} + 2\mathbf{c}$ . (b) Determine the unit vector  $\mathbf{u}$  that is parallel to this vector.

2.8 Suppose a vector runs from the point (1, 2, 1) to another point (-1, -2, 3). Write the expression for this vector in rectangular form.

2.9 Suppose  $\mathbf{a} = 3\mathbf{i} + 2\mathbf{j} - 5\mathbf{k}$  and  $\mathbf{b} = 2\mathbf{i} - \mathbf{j} - \mathbf{k}$ . (a) Find  $\mathbf{a} \cdot \mathbf{b}$ , and (b)  $\mathbf{a} \times \mathbf{b}$ . (c) Are these vectors perpendicular to each other? (d) Are they parallel or antiparallel to each other?

2.10 Find the angle between  $\mathbf{a} = 2\mathbf{i} - 3\mathbf{j} - \mathbf{k}$  and  $\mathbf{b} = 4\mathbf{k}$ .

2.11 Show that  $2\mathbf{i} - 6\mathbf{j} + 3\mathbf{k}$  is normal to  $3\mathbf{i} - 2\mathbf{j} - 6\mathbf{k}$ .

2.12 Find a unit vector  $\mathbf{u}$  that is perpendicular to the vector  $3\mathbf{i} - 2\mathbf{j} - 5\mathbf{k}$  when the  $z$  component of  $\mathbf{u}$  is zero; that is, when  $u_z = 0$ .

2.13 (a) Find a unit vector  $\mathbf{u}$  that is parallel to the vector  $3\mathbf{i} - 2\mathbf{j} - 5\mathbf{k}$ ; (b) antiparallel to the vector.

2.14 Do the algebraic work to obtain Equation 2.19.

2.15 Show all the algebraic steps required to derive Equation 2.35.

2.16 Show how to obtain Equation 2.37.

2.17 Draw a diagram for a concave surface and show that Equation 2.43c holds for such a surface. To guide you, look at how Equation 2.41 was obtained.

2.18 Put in the steps to derive Equation 2.52b.

2.19 Put in the steps to derive Equation 2.52c.

2.20 Write a computer program in the software language of your choice to implement the flow chart in Figure 2.19 and reproduce the results of Example 2.3.1.

2.21 With the results of Problem 2.20, (a) determine if the rectangular coordinates  $x_1, y_1, z_1$  on surface 1 satisfy Equation 2.38, and (b) determine if the direction cosines satisfy Equation 2.53. (c) Do the same for the rectangular coordinates on surface 2, and (d) for the direction cosines on that surface. Because of roundoff error, you might not get the exact values predicted by Equations 2.38 and 2.53, but they should be very close.

2.22 Use the program that you developed in Problem 2.20 to exactly trace the ray in Example 1.3.1. The properties of the lens are given in Figure 2.57. You must change the  $\delta$  value to  $\alpha, \beta, \gamma$  values.

|                                      | $r$ (mm) | $n$   | $t$ (mm) |
|--------------------------------------|----------|-------|----------|
| $\delta = 0.100$ rad<br>$= 5.73$ deg | 40.00    | 1.000 | 60.00    |
|                                      | -40.00   | 1.500 | 20.00    |
| $y = 5.00$ mm                        |          | 1.000 | 40.00    |
|                                      | $\infty$ |       |          |

Figure 2.57

2.23 Similar to Problem 2.22 except the lens is the diverging one of Example 1.3.3. The data is given in Figure 2.58.

|  | $r$ (mm) | $n$   | $t$ (mm) |
|--|----------|-------|----------|
| $\delta = -0.127$ rad<br>$= -7.28$ deg | -40.00   | 1.000 | 50.00    |
|  | 40.00    | 1.500 | 10.00    |
| $y = 14.00$ mm                         |          | 1.000 | 56.00    |
|  | $\infty$ |       |          |

Figure 2.58

2.24 Trace the ray exactly with the data given in Figure 2.59 for the doublet discussed in Example 1.3.5.

|                                      | $r$ (mm) | $n$    | $t$ (mm) |
|--------------------------------------|----------|--------|----------|
| $\delta = 0.110$ rad<br>$= 6.30$ deg | 90.17    | 1.0000 | 60.00    |
|                                      | -90.17   | 1.5166 | 7.62     |
| $y = 7.00$ mm                        |          | 1.6256 | 5.08     |
|                                      | -1524.00 | 1.0000 | 50.00    |
|                                      | $\infty$ |        |          |

Figure 2.59

2.25 In this problem the ray does not start in the  $yz$  plane, but is more like Problem 2.20. Use the data in Figure 2.60 to trace the ray exactly.

|                                       | $r$ (mm) | $n$   | $t$ (mm) |
|---------------------------------------|----------|-------|----------|
| $P : x = 10$ mm<br>$y = 1$<br>$z = 2$ | 50.00    | 1.000 | 10.00    |
|                                       | -50.00   | 1.500 | 15.00    |
| $\alpha = -0.1$<br>$\beta = 0.1$      |          | 1.000 | 20.00    |
|                                       | $\infty$ |       |          |

Figure 2.60

2.26 Use Example 2.4.1 as a guide to write a program that modifies the basic flow chart in Figure 2.19 so that it calculates  $\ell'_F$  with the appropriate paraxial equations from Chapter 1. Also, include in your program Equations 2.54 for calculating TSA, LSA, and  $t'$ . Then use your program to reproduce the table in Figure 2.29.

2.27 Show how to get the  $c$  form in Equation 2.55 starting with the  $r$  form.

2.28 Show the steps in deriving Equations 2.57.

2.29 Using Equation 2.55, (a) show that  $S \rightarrow -1$  as  $c_1 \rightarrow 0$ . (b) Show in a similar way that  $S \rightarrow 1$  as  $c_2 \rightarrow 0$ .



- 2.30** Using Equation 2.55, (a) show that  $S \rightarrow -1$  as  $r_1 \rightarrow \infty$ .  
(b) Show in a similar way that  $S \rightarrow 1$  as  $r_2 \rightarrow \infty$ .
- 2.31** Write a computer program that implements the flow chart in Figure 2.41 and obtain the TSA versus  $S$  graph of Figure 2.42. Also determine the values of TSA,  $S$ , and  $c_1, c_2, r_1, r_2$  at the point where TSA is a maximum; that is, obtain the values above the graph of Figure 2.42.
- 2.32** Modify an appropriate program to get the angles shown in Figure 2.43.
- 2.33** Show how to obtain Equations 2.60a and 2.60b from Equations 2.59.
- 2.34** Use Equations 2.60 to obtain Equation 2.61.
- 2.35** Use both Equations 2.60 and Equation 2.61 to calculate the radius  $R$  of the converging lens given in the table of Figure 2.57.
- 2.36** Use the program you developed in Problem 2.26 to obtain the values in Figure 2.51 and the graph in Figure 2.52.
- 2.37** Use the program you developed in Problem 2.26 to obtain the values in Figure 2.55 and the graph in Figure 2.56.

## Chapter 2: Answers to Problems

Note: All the calculations are made with *Mathematica's* 16 decimal digit precision and the results are displayed to six decimal digits, unless the digits to the right of the decimal point are trailing zeros, then they are not printed.

- 2.1** (a)  $-0.5$ ,  $0.642788$ ,  $0.580366$
- 2.2** (a)  $0.0707372$ ,  $0.777573$ ,  $0.624801$
- 2.3** (a)  $0.707107$ ; (b)  $60$  deg,  $60$  deg,  $45$  deg
- 2.4** (a)  $60$  deg
- 2.5** (a)  $0$  deg,  $90$  deg,  $90$  deg; (b)  $1$ ,  $0$ ,  $0$
- 2.6** (a)  $3.74166$ ; (b)  $0.534522 \mathbf{i} - 0.267261 \mathbf{j} - 0.801784 \mathbf{k}$ ;  
(c)  $0.534522$ ,  $-0.267261$ ,  $-0.801784$ ;  
(d)  $57.6885$  deg,  $105.501$  deg,  $143.301$  deg
- 2.7** (a)  $11.7898$ ; (b)  $0.254457 \mathbf{i} + 0.593732 \mathbf{j} - 0.76337 \mathbf{k}$
- 2.8**  $-2 \mathbf{i} - 4 \mathbf{j} + 2 \mathbf{k}$
- 2.9** (a)  $9$ ; (b)  $-7 \mathbf{i} - 7 \mathbf{j} - 7 \mathbf{k}$
- 2.10**  $105.501$  deg
- 2.12**  $0.5547 \mathbf{i} + 0.83205 \mathbf{j}$
- 2.13** (a)  $0.486664 \mathbf{i} - 0.324443 \mathbf{j} - 0.811107 \mathbf{k}$ ;  
(b)  $-0.486664 \mathbf{i} + 0.324443 \mathbf{j} + 0.811107 \mathbf{k}$

Note: To make it easier to interpret the answers to the exact ray tracing problems, we key the results to the surfaces with subscripts—except for the initial and last surfaces, there we use unprimed and primed symbols, respectively.

- 2.20** Units for rectangular coordinates in mm:  
 $x = 2$ ,  $y = 1$ ,  $z = 2$ ;  
 $\alpha = 0.2$ ,  $\beta = 0.2$ ,  $\gamma = 0.959166$   
 $x_1 = 3.78485$ ,  $y_1 = 2.78485$ ,  $z_1 = 0.559848$ ;  
 $\alpha_1 = 0.064202$ ,  $\beta_1 = 0.0824673$ ,  $\gamma_1 = 0.994524$   
 $x_2 = 3.98453$ ,  $y_2 = 3.04134$ ,  $z_2 = -1.34704$ ;  
 $\alpha_2 = -0.135022$ ,  $\beta_2 = -0.0528661$ ,  $\gamma_2 = 0.989431$   
 $x' = 2.16314$ ,  $y' = 2.32819$ ,  $z' = 0$

- 2.22** Units for rectangular coordinates in mm:  
 $x = 0$ ,  $y = 5$ ,  $z = 0$ ;  
 $\alpha = 0$ ,  $\beta = 0.0998334$ ,  $\gamma = 0.995004$   
 $x_1 = 0$ ,  $y_1 = 11.18$ ,  $z_1 = 1.59418$ ;  
 $\alpha_1 = 0$ ,  $\beta_1 = -0.0313054$ ,  $\gamma_1 = 0.99951$   
 $x_2 = 0$ ,  $y_2 = 10.6488$ ,  $z_2 = -1.4435$ ;  
 $\alpha_2 = 0$ ,  $\beta_2 = -0.189872$ ,  $\gamma_2 = 0.981809$   
 $x' = 0$ ,  $y' = 2.634$ ,  $z' = 0$

- 2.23** Units for rectangular coordinates in mm:  
 $x = 0$ ,  $y = 14$ ,  $z = 0$ ;  
 $\alpha = 0$ ,  $\beta = -0.126659$ ,  $\gamma = 0.991946$   
 $x_1 = 0$ ,  $y_1 = 7.71145$ ,  $z_1 = -0.750369$ ;  
 $\alpha_1 = 0$ ,  $\beta_1 = -0.0179253$ ,  $\gamma_1 = 0.999839$   
 $x_2 = 0$ ,  $y_2 = 7.50598$ ,  $z_2 = 0.710557$ ;  
 $\alpha_2 = 0$ ,  $\beta_2 = 0.0690435$ ,  $\gamma_2 = 0.997614$   
 $x' = 0$ ,  $y' = 11.3325$ ,  $z' = 0$

- 2.24** Units for rectangular coordinates in mm:  
 $x = 0$ ,  $y = 7$ ,  $z = 0$ ;  
 $\alpha = 0$ ,  $\beta = 0.109778$ ,  $\gamma = 0.993956$   
 $x_1 = 0$ ,  $y_1 = 13.7431$ ,  $z_1 = 1.05347$ ;  
 $\alpha_1 = 0$ ,  $\beta_1 = 0.0192682$ ,  $\gamma_1 = 0.999814$   
 $x_2 = 0$ ,  $y_2 = 13.849$ ,  $z_2 = -1.06987$ ;  
 $\alpha_2 = 0$ ,  $\beta_2 = 0.0283627$ ,  $\gamma_2 = 0.999598$   
 $x_3 = 0$ ,  $y_3 = 14.0217$ ,  $z_3 = -0.0645053$ ;  
 $\alpha_3 = 0$ ,  $\beta_3 = 0.0403488$ ,  $\gamma_3 = 0.999186$   
 $x' = 0$ ,  $y' = 16.0434$ ,  $z' = 0$

- 2.25** Units for rectangular coordinates in mm:  
 $x = 10$ ,  $y = 1$ ,  $z = 2$ ;  
 $\alpha = -0.1$ ,  $\beta = 0.1$ ,  $\gamma = 0.989949$   
 $x_1 = 9.10376$ ,  $y_1 = 1.89624$ ,  $z_1 = 0.872351$ ;  
 $\alpha_1 = -0.127884$ ,  $\beta_1 = 0.0539155$ ,  $\gamma_1 = 0.990323$   
 $x_2 = 7.35876$ ,  $y_2 = 2.63193$ ,  $z_2 = -0.61456$ ;  
 $\alpha_2 = -0.269914$ ,  $\beta_2 = 0.0529444$ ,  $\gamma_2 = 0.961428$   
 $x' = 1.57136$ ,  $y' = 3.76714$ ,  $z' = 0$

## References

1. Donald P. Feder, "Optical Calculations with Automatic Computing Machinery," *Journal of the Optical Society of America* **41**, 630 (1951).  
One of the first articles to describe equations used for computer calculations.
2. Warren J. Smith, *Modern Optical Engineering*, 3rd edition, McGraw-Hill, New York, 2000.  
One of the basic textbooks of lens design.